Distribution Agreement

In presenting this thesis as a partial fulfillment of the requirements for a degree from Emory University, I hereby grant to Emory University and its agents the non-exclusive license to archive, make accessible, and display my thesis in whole or in part in all forms of media, now or hereafter now, including display on the World Wide Web. I understand that I may select some access restrictions as part of the online submission of this thesis. I retain all ownership rights to the copyright of the thesis. I also retain the right to use in future works (such as articles or books) all or part of this thesis.

Roger Tieu April 15, 2015

Targeting TIM-3 to reverse immune exhaustion during chronic viral infection

By

Roger Tieu

Francois Villinger, DVM/PhD

Adviser

Department of Pathology and Laboratory Medicine

Francois Villinger, DVM/PhD

Adviser

Elena Conis, PhD

Committee Member

Arri Eisen, PhD

Committee Member

David Lynn, PhD

Committee Member

Emily Weinert, PhD

Committee Member

April 15, 2015

Targeting TIM-3 to reverse immune exhaustion during chronic viral infection

By

Roger Tieu

Francois Villinger, DVM/PhD

Adviser

An abstract of
a thesis submitted to the Faculty of Emory College of Arts and Sciences
of Emory University in partial fulfillment
of the requirements of the degree of
Bachelor of Sciences with Honors

Department of Biology

2015

Abstract

Targeting TIM-3 to reverse immune exhaustion during chronic viral infection
By Roger Tieu

Human immunodeficiency virus infection and acquired immune deficiency syndrome (HIV/AIDS) have emerged as a major threat by being able to impair the immune system. Though the exact mechanism of disease pathogenesis is not clear, several inhibitory receptors involved in effector mechanisms are invoked by the chronic HIV infection leading to limited antiviral response. TIM-3 (T cell immunoglobulin and mucin domain 3) has been identified as an important albeit still understudied negative regulatory of immunity. In order to characterize TIM-3 in the context of chronic viral infection, we used SIV-infected rhesus macaques as our model system. We find there is a similar frequency of TIM-3 expressing dendritic cells (DCs) between humans and rhesus macaques. Further characterization of TIM-3 expressing DCs revealed they represent an activated population with increased CD86 expression and secreted tumor necrosis factor alpha (TNF-α) in response to the presence of dsRNA (double stranded RNA). We also find an increased concentration of soluble galectin-9, a TIM-3 ligand, in plasma samples after SIV infection. Staining for general TIM-3 ligands revealed their presence on various immune cell populations, including T cells, B cells, monocytes, and DCs. Finally, we created a fusion protein of extracellular TIM-3 and the Fc domain of an IgG2 antibody to generate TIM-3-Fc for blocking TIM-3 signaling. Treatment of peripheral blood mononuclear cells with TIM-3-Fc results in enhanced proliferation of antigen-specific $CD4^+$ T cells in vitro. Overall, these findings reveal a need to further characterize TIM-3 since we establish TIM-3 as not only an inhibitory molecule for adaptive immunity, but also an activation molecule for innate immunity.

Targeting TIM-3 to reverse immune exhaustion during chronic viral infection

By

Roger Tieu

Francois Villinger, DVM/PhD

Adviser

A thesis submitted to the Faculty of Emory College of Arts and Sciences
of Emory University in partial fulfillment
of the requirements of the degree of
Bachelor of Sciences with Honors

Department of Biology

2015

Acknowledgements

This study was supported by grants from the National Institute of Health (RO1 AI078775 and 8R24 OD010947) to Francois Villinger, DVM/PhD, and (R01 AI113883) to Siddappa N. Byrareddy, PhD.

I owe many thanks to my research mentors Praveen Amancha, Kenneth Rogers, and Francois Villinger, for their guidance and support throughout this study. Since walking through his door for the first time holding a research proposal, Francois has always provided his support, shared his wisdom, and demonstrated his belief in me. Also, Ken has always been there to answer my many questions ranging from the nitty-gritty details of how a specific technique works to my own curiosities such as why a B cell is called a B cell. Finally, I am grateful for my mentor Praveen who has played a fundamental role in my research career. Since my first day in the lab, Praveen took me under his wing and taught me the workings of immunology research. He has continued to motivate me through the daily struggles of the research life, demonstrating that the journey is all worth the effort.

I would like to thank Balwan Singh and Guofu Fang for technical assistance as well as the members of the Villinger Lab for their various and invaluable discussions that include operating million dollar lasers and baking caffeinated desserts. I would like to also thank Sid for collaborating with us and sharing his work with galectin-9. It has been an honor to carry out research in this lab and I am fortunate to have had this opportunity to be surrounded by those who love science and life.

I would also like to acknowledge the enormous role that my advisors played in my personal and professional development throughout college. Dr. Jose Soria introduced a freshman kid to the world of organic chemistry, and taught him the importance of enjoying a good laugh and community. Dr. David Lynn taught me the importance of asking questions and figuring out how to go about answering those questions in an ORDER-ly way. Dr. Arri Eisen showed me the importance of expanding my focus of science to encompass society as a whole. Dr. Elena Conis introduced me to the history of vaccines and taught me how I must view global health from multiple perspectives. Dr. Emily Weinert introduced me to the exciting field of chemical biology and gave me the confidence that my crazy ideas may actually work.

Finally, I would like to thank my mom, dad, grandparents, and all of my family and friends for all of their love, support, and encouragement as I continue on my adventure of life. To my friends back home, distance can never separate us and we will always be troublemakers. To my friends at Emory and beyond, the memories we made and continue to make together will guide us for the days to come as we strive to take on the world. To my bud Pika, well, we still have a lot more to do so let's hit up some coffee and prepare for another chapter.

Table of Contents

List of Figures

Introduction

Background

The immune system represents a highly evolved biological system capable of learning, memory, and pattern recognition between self and foreign. Cells of the innate immune system detect and respond to the presence of non-self entities, such as pathogens and their associated components such as protein (antigen), through pattern recognition receptors (1). This response generates an environment promoting the activation of antigen presenting cells (APCs), which initiate the elaboration of specific adaptive immunity through a complex network of stimulatory and inhibitory signals (2). The initial response by both T and B cells requires two signals: 1) an antigen-specific signal delivered via the T or B cell receptor; and 2) a second co-stimulatory signal to initiate a productive activation and proliferation of effector cells with the intent of eliminating the invading pathogen. After removing the threat, feedback loops limit both the inflammatory response and the expansion of such effector cells primarily via apoptosis, but leave in place cells with long-term memory, a mechanism induced also by immunization.

Immune System Overview

The overall immune system can be classically divided into innate and adaptive immunity. The innate immune system represents a population equipped with non-specific defense mechanisms that can rapidly activate either immediately or within hours of a foreign entity entering the body. The adaptive immune system utilizes an antigen-specific specific response that develops over a longer period time where a specialized and specific population of cells proliferates and attacks that specific antigen. Generally speaking, the

innate immune population consists of the phagocytic cells (neutrophils, monocytes, and macrophages) that actively engulf antigen, the inflammatory mediators (basophils, eosinophils, and mast cells) that secrete molecules promoting inflammation, and the natural killer (NK) cells (Fig. 1).

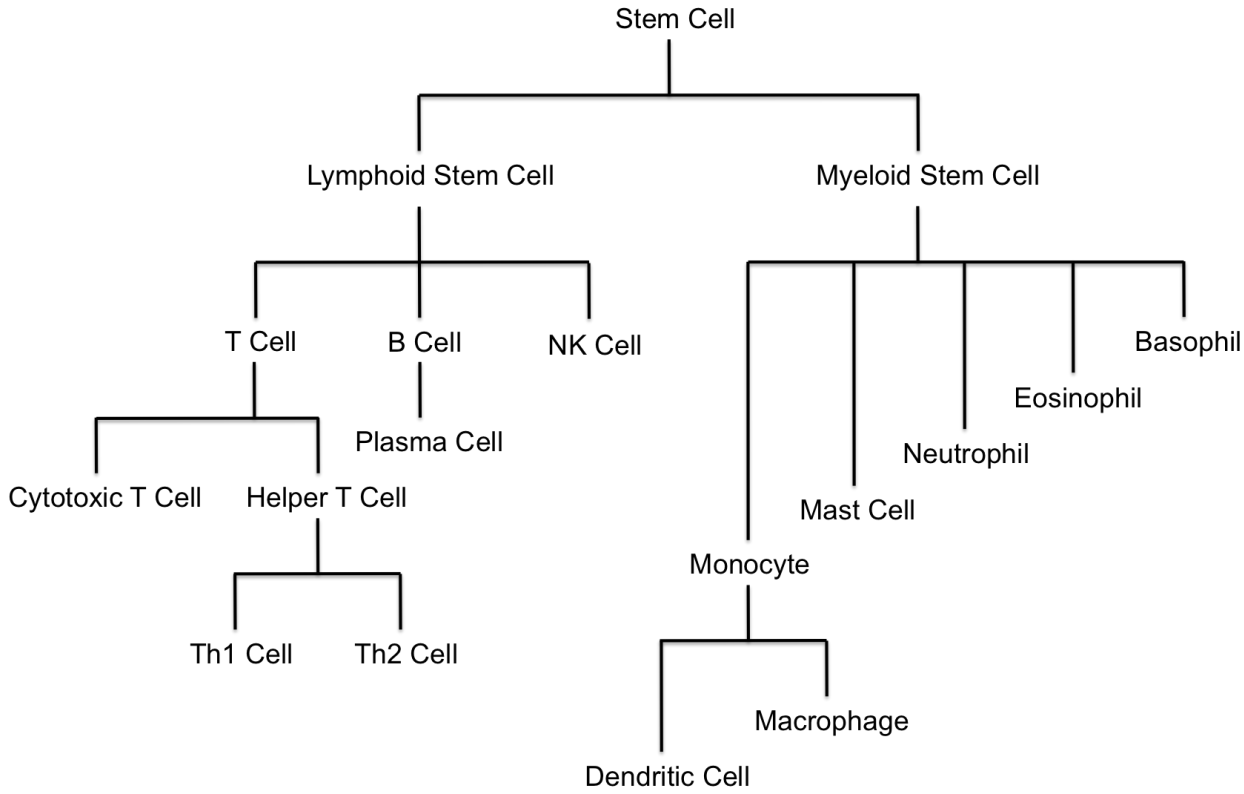

Figure 1. General origin and differentiation of cells from the immune system. Depending on the environment, timing, and signaling patterns, a multipotential hematopoietic stem cell will follow a specific genetic programing and differentiate into one of the listed types of immune cells.

The adaptive immune population consists of the T and B cells (Fig. 1) that upon binding of antigen to their T cell receptor (TCR) or B cell receptor (BCR), respectively, will mediate an antigen-specific response. Upon activation, B cells specific to the antigen

proliferate and mature into plasma cells that secrete out antigen-specific antibodies. Antibodies serve to block antigen-expressing pathogens from infecting additional cells as well as to mark the pathogen as a target for other immune cells. Specifically, T cells can be subdivided into $CD4^+$ T cells, also known as "helper" T cells which support other immune cells, and $CD8^+$ T cells, also known as cytotoxic or "killer" T cells which actively kill cells. The $CD4^+$ T cells can be further subdivided into the Th1 population, which secrete interleukin-2 (IL-2) and interferon-gamma (IFN-γ) to promote cellular immunity (i.e. the activation of $CD8^+$ T cells and NK cells), and into the Th2 population, which secrete IL-4, IL-10 and IL-13 to promote humoral immunity (i.e. the activation of B cells for antibody secretion). Upon antigen clearance, those antigen-specific T and B cells can mature into memory T cells and B cells, respectively. A second encounter with a pathogen expressing those same antigens will activate these memory cells that can mediate a quicker and stronger recall immune response.

Typically, the innate and adaptive immune systems work together to eliminate pathogens from the body. The key players in mediating this cooperation are the dendritic cells (DCs). DCs constantly but quietly roam the body and endocytose antigens. However, they become activated when an extracellular or intracellular pattern-recognition receptor recognizes a distinctive pathogen-associated antigen. Activation causes DCs to maturate and express co-stimulatory molecules to provide activation signals for T and B cells. In addition, activated DCs process the antigen and present fragments complexed within the major-histocompatibility-complex (MHC) molecules on the cell surface to prime and activate T and B cells specific to the presented antigen. As outlined above, complete

activation of T or B cells requires a secondary signal such as CD80/86 on DCs interacting with CD28 on T cells (3).

Immune exhaustion

During the course of cancer and chronic viral infections, where the pathogen is not eliminated, antigen stimulation persists, yet the regulatory feedback loops are engaged. By preventing a return to normalcy, immune dysfunction and dysregulation arises, resulting in the generation of 'exhausted' effector cells with poor function (4). This impairment has been associated with prolonged inhibitory signaling that normally minimizes collateral damage during inflammation and prevents autoimmunity by maintaining self-tolerance, but in the context of chronic infection, limits the ability of the host to combat the infection further. Among the dysfunctional are T cells in a phenomenon known as T cell exhaustion (4).

T cell exhaustion describes a progressive loss of function in pathogen-specific $CD4^+$ and $CD8^+$ T cells in a hierarchical manner with impaired production of IL-2 as well as cytotoxicity and proliferation, followed by loss of TNF-α, and eventually IFN-γ at late stages (4). This exhaustion has been found to be associated with prolonged and overexpression of multiple inhibitory receptors in concert with their ligands that are also upregulated on APCs. The first such regulatory molecule discovered was CTLA-4, which binds CD80/CD86 with an approximately 10-fold higher affinity than CD28 (5, 6), leading to its use in the context of organ transplantation (7).

Another study using the mouse model of chronic LCMV (lymphocytic choriomeningitis virus) infection, revealed that PD-1 (programmed death 1) was

selectively upregulated by exhausted T cells, and blocking interactions of this inhibitory receptor with its ligands using antibodies enhanced virus-specific $CD8^+$ T cell response and decreased viral load (8). This finding highlighted the potency of such individual inhibitory pathways in controlling T cell response in chronic viral infection as well as the potential for targeting these same pathways. However, blockade of the PD-1 pathway only partially restored T cell function, indicating the involvement of other inhibitory pathways. Additional inhibitory receptors include B and T lymphocyte attenuator (BTLA), lymphocyte activation gene 3 (LAG-3), T cell immunoglobulin and mucin domain 3 (TIM-3), CD244 (2B4), and killer cell lectin like receptor G1 (KLRG1) (9-14).

The inhibitory receptor TIM-3

TIM-3 is a type I transmembrane protein consisting of an N-terminal immunoglobulin variable (IgV)-like domain, a mucin domain with potential sites of O- and N-linked glycosylation, followed by a transmembrane domain, and a cytoplasmic tail with tyrosine phosphorylation motifs. Attempts to identify new Th1 specific cell surface proteins resulted in the identification of TIM-3. Treatment with antibody raised against TIM-3 exacerbated experimental autoimmune encephalomyelitis (EAE) in mice (15), suggesting its role in peripheral tolerance and prevention of autoimmunity which was supported in later studies (16, 17). Elevated TIM-3 expression was found on dysfunctional T cells from HIV-infected individuals, and blockade of TIM-3 with antibody or soluble TIM-3 enhanced function of HIV-specific T cells, implicating the role of TIM-3 as an inhibitory receptor (12).

The TIM-3 ligand, galectin-9

Galectin-9 was identified as a ligand binding to the carbohydrate motifs on the IgV domain of murine TIM-3 (18). Interaction of galectin-9 with TIM-3 expressing Th1 cells induced their apoptosis. Given the nature of TIM-3/galectin-9 interactions, much effort has focused on identifying a specific galectin-9 expressing population. Initial reports have found regulatory T cells (Tregs) and naïve $CD4^+$ T cells to express galectin-9 (19, 20), though additional studies will be needed to elucidate in what context galectin-9 assumes an active role. In addition, select functions involving TIM-3 have strongly suggested the existence of other yet to be determined TIM-3 ligands.

Role of TIM-3 in chronic viral infections

Increased expression of TIM-3 has been observed on exhausted $CD8^+$ T cells isolated from humans infected with human immunodeficiency virus (HIV) (12, 21, 22), hepatitis B virus (HBV) (23, 24), and hepatitis C virus (HCV) (21, 25, 26) as well as in murine models of HBV (27), herpes simplex virus (HSV) (28) and LCMV infection (29), and in SIV-infected rhesus macaques (30, 31). Even though chronic stimulation by viral presence has been associated with elevated expression of TIM-3, HIV infection of $CD4^+$ T cells does not induce expression of TIM-3 on T cells (32). Instead, TIM-3 expression increases indirectly via TCR/CD28 co-stimulation, which provides evidence for the role of TIM-3 to restrain effector response in a temporal fashion.

During chronic viral infections with sustained antigen stimulation, exhausted $CD8^+$ T cells can co-express multiple inhibitory receptors, which can work synergistically to modulate the functional quality of these virus-specific $CD8^+$ T cells (14). The severity of

exhaustion tends to correlate with the combined number of expressed inhibitory receptors. Co-expression of TIM-3 and PD-1 on $CD8^+$ T cells in a murine model of LCMV had an association with severe $CD8^+$ T cell exhaustion with respect to diminished proliferation and cytokine production (29). TIM-3 and PD-1 work synergistically as evident with TIM-3 blockade or PD-1 blockade alone partially restoring T cell effector function, but upon dual blockade, T cell function restoration was significantly greater than the additive effects of TIM-3 or PD-1 blockade alone. A mechanism for the role of inhibitory TIM-3 has been proposed (Fig. 2).

SIV-infected rhesus macaques, a model for AIDS

Non-human primate models have been widely used to study the pathogenesis of HIV/AIDS as well as for the development of vaccine and therapeutic treatments. In rhesus macaques of Indian origin, simian immunodeficiency virus (SIV) infection follows a similar disease course as HIV infection of humans making them an ideal model (33).

Immune exhaustion has been described in chronically SIV-infected rhesus macaques (31, 34, 35). With the initial identification of PD-1 as an inhibitory receptor, SIV-infected rhesus macaques were treated with a humanized anti-PD-1 monoclonal antibody as an immunotherapeutic treatment to block PD-1 signaling (34). Overall, T and B cell functions were improved, viral loads decreased, and animal survival rates were increased. However, the level of anti-PD-1 antibody declined rapidly due to an antibody response against the xenobiotic partially humanized mouse antibody. With these limitations in mind, a recombinant PD-1 receptor fused to Ig-Fc has been generated to block PD-1 signaling (35). Such a molecule would prevent binding of PD-1 to its ligands. In vitro use of PD-1-Fc

improved SIV-specific $CD4^+$ and $CD8^+$ T cell proliferation. Furthermore, in vivo administration of PD-1-Fc to SIV-infected rhesus macaques was found to be safe and non-immunogenic as repeat administrations of PD-1-Fc did not elicit an antibody response and PD-1 blockade with PD-1-Fc in conjunction with ART interruption resulted in a significant albeit transient delay in viral rebound.

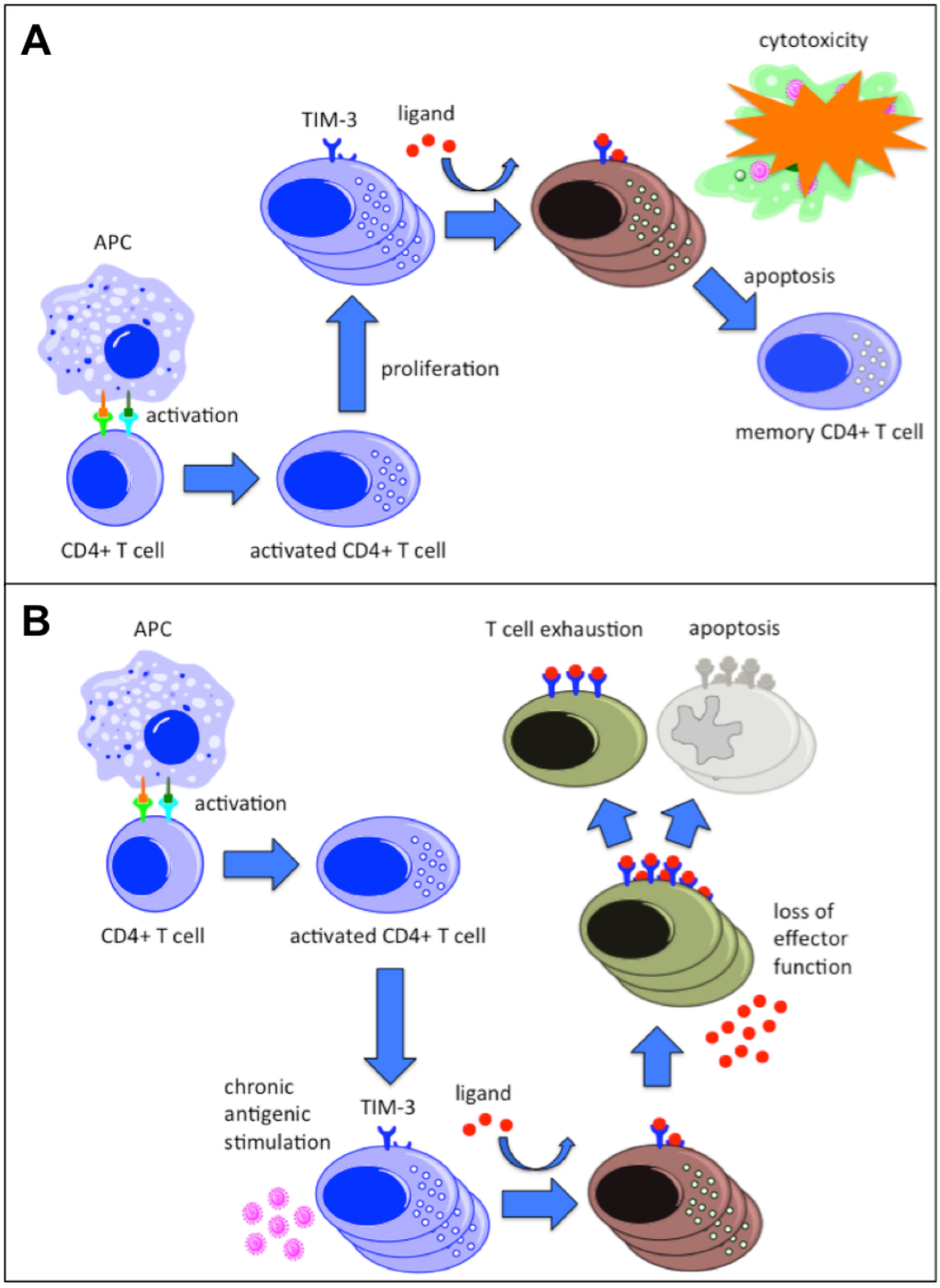

Figure 2. Proposed mechanism for TIM-3 in modulating T cell function. (A) Acute infection where CD4⁺ T cells proliferate and mediate the clearance of invading pathogens, and upon removing the threat, TIM-3 signaling restrains CD4⁺ T cell response and eliminates many through apoptosis, while a fraction become long-term memory cells. **(B)** Chronic infection where CD4⁺ T cells are constantly stimulated by antigen, resulting in the upregulation of TIM-3 which strengthens inhibitory signaling and leads to either T cell exhaustion or apoptosis.

Objectives

The following represent the experimental objectives of this study:

1. Identify the expression pattern of TIM-3 on the various immune cell populations
    a. Flow cytometric analysis using cell surface markers (CD3, CD4, CD8, CD11c, CD14, CD16, CD20, CD28, CD95, CD123, HLA-DR, NKG2A, PD-L2, and TIM-3) (Fig. 3) to define distinct populations
    b. Characterize the $CD11c^{+}$ mDC population for functional response
2. Establish a baseline of galectin-9 amongst naïve and SIV-infected rhesus macaques
    a. Quantify plasma levels of galectin-9
    b. Identify cell populations expressing galectin-9
3. Construct Fc fusions of extracellular TIM-3 as well as the various splice variants
    a. Production of recombinant proteins TIM-3-Fc, IgV-Fc, and mucin-Fc
4. Identify immune cell populations expressing TIM-3 ligand
    a. Flow cytometric analysis using TIM-3-Fc in addition to cell surface markers
5. Reverse T cell exhaustion by blocking TIM-3 signaling
    a. Measure proliferative capacity

Methods

Ethics statement

All animals were born and maintained at the Yerkes National Primate Research Center of Emory University in accordance with the regulations of the Committee on the Care and Use of Laboratory Animal Resources. The animals are fed monkey diet (Purina) supplemented daily with fresh fruit. Additional enrichment is provided and overseen by the Yerkes staff and animal health is monitored daily by the animal care staff and veterinary personnel. Animals that reached IACUC defined endpoints, including pain or stress that could not be alleviated therapeutically were humanely euthanized with an overdose of barbiturate consistent with the recommendation of the American Veterinary Medical Association. All experiments were reviewed and approved by the Emory Institutional Animal Care as well as Biosafety Committee. Animals were inoculated with 200 $TCID_{50}$ (50% tissue culture infective dose) of SIVmac239 intravenously and served as a source of blood at various time points post-infection. Human blood was obtained from healthy donors after providing written informed consent, and the protocol was approved by the Institutional Review Board of Emory University.

Flow cytometric analysis

PBMCs (peripheral blood mononuclear cells) were isolated from freshly obtained peripheral blood samples from each rhesus monkey or from humans using standard Ficoll-Hypaque gradient centrifugation. Briefly, 1 x 10^6 PBMCs were used for multi parameter flow cytometer staining. For panel 1, the antibody cocktail mix was against CD3 (SP34-2), CD4 (L200), CD8 (RPA-T8), CD20 (L27), CD28 (CD28.2), CD95 (DX2), HLA-DR (TU36),

NKG2A (Z199, Beckman Coulter) and TIM-3 (344823, PE-conjugate, R&D or isotype Rat IgG2A-PE) and for panel 2, the antibody cocktail mix was against (CD3, CD8, CD20 in APC-Cy7), CD14 (M5E2), CD16 (3G8), HLA-DR (TU36), CD123 (7G3), CD11c (3.9), PD-L2 (24F.10C12) and TIM-3 (344823, PE-conjugate, R&D or isotype Rat IgG2A-PE), were added and incubated at 37°C in the dark for 30 minutes. At the end of incubation, PBMCs were washed with 2% FBS in PBS (FACS wash solution), centrifuged, and supernatant was discarded. PBMCS were fixed in 1% PFA (paraformaldehyde) and acquired on a LSRII flow cytometer (BD Biosciences) driven by the FACS DiVa software. Analysis of the acquired data was performed using FlowJo software (version 9.2; TreeStar, Ashland, OR). The gating strategy is illustrated (Fig. 3) and the phenotype of the various cell subsets analyzed in this study are illustrated (Fig. 4).

For intracellular galectin-9 staining, PBMCs were permeabilized in BD Fixation and Permeabilization Solution (#554722, BD Biosciences) at 4°C for 20 minutes in the dark, and then washed with BD Permeabilization Wash Buffer (#554723, BD Biosciences) added directly to the tube. Then, anti-galectin-9 (9M1-3) was added to the permeabilized cells, incubated at 40°C for 30 minutes in the dark, and then washed with FACS wash solution. Finally, PBMCs were fixed in 1% PFA and acquired on a LSRII flow cytometer (BD Biosciences).

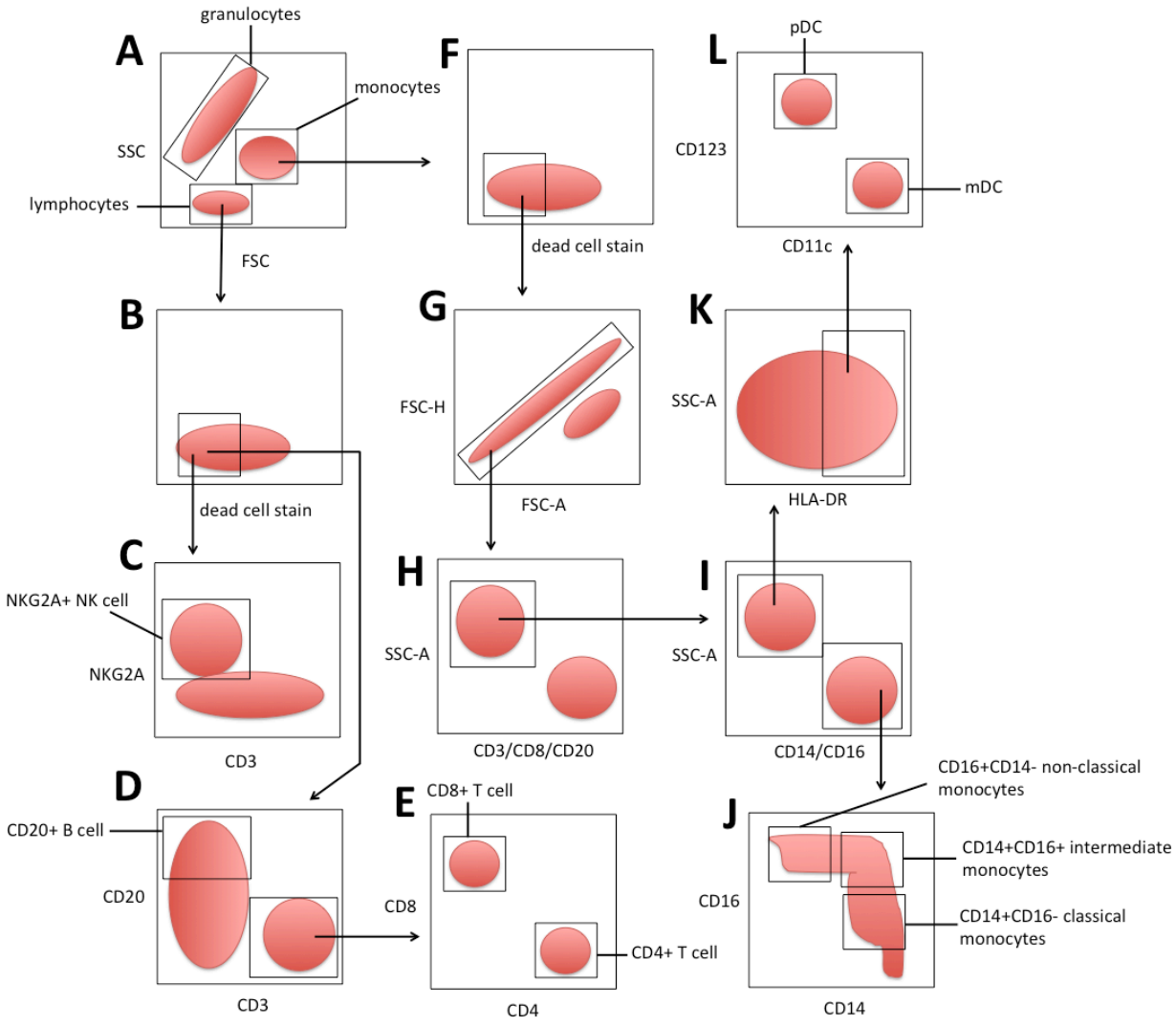

Figure 3. Flow cytometry gating strategy for PBMCs. (A) Forward scatter (FSC) measures the diameter of the cell and side scatter (SSC) measures the granularity of the cell. **(B)** Lymphocytes are gated through dead cell staining to analyze only viable cells. **(C)** Lymphocyte gating on lineage markers CD3 and NKG2A reveals the $CD3^{-}NKG2A^{+}$ NK cell population. **(D)** Lymphocyte gating on lineage markers CD3 and CD20 reveals the CD20+ B cells and CD3+ T cells. **(E)** T cell gating reveals two distinct populations consisting of the CD4+ T cells and CD8+ T cells. **(F)** Monocytes are gated through dead cell staining to analyze only viable cells. **(G)** Monocytes are gated through FSC-A and FSC-H to discriminate doublets from single cells where everything within the diagonal box is considered single cells. **(H)** Gating on lineage markers CD3/CD8/CD20 allows for analyzing populations lacking those markers. **(I)** Cells that are negative for lineage markers CD3/CD8/CD20 can be further gated for the expression of lineage markers CD14/CD16. **(J)** Monocyte gating reveals three distinct populations consisting of $CD16^{+}CD14^{-}$ non-classical monocytes, $CD14^{+}CD16^{+}$ intermediate monocytes, $CD14^{+}CD16^{-}$ classical monocytes. **(K)** Cells that are

negative for lineage markers CD14/CD16 can be further gated for the expression of lineage marker HLA-DR to identify the DC population. **(L)** DC dating reveals two distinct populations consisting of the $CD123^+$ plasmacytoid DCs (pDCs) and $CD11c^+$ myeloid DCs (mDCs).

TLR stimulation

Briefly, 1 x 10^6 PBMCs were stimulated with Toll-like receptor (TLR) agonists, specifically TLR-3 (poly IC, 10μg/ml) and TLR-4 (MPL, 125ng/ml) agonists in the presence of brefeldin A (10 μg/ml) for 5 hours at 37°C, 7%CO_2. PBMCs were then stained for Live/Dead marker followed by antibody cocktail mix of surface markers against (CD3, CD8, CD20 in APC-Cy7), CD14, CD16, HLA-DR, CD123, CD11c, PD-L2 and TIM-3. Following permeabilization (BD kit), PBMCs were stained with anti-TNF-α (MAb11), anti-IL-12/IL-23 p40 (C8.6). Finally, PBMCs were fixed in 1% PFA and acquired on LSRII flow cytometer (BD Biosciences). Analysis of the acquired data was performed using FlowJo software (version 9.2; TreeStar).

Detection of galectin-9 in plasma

Galectin-9 was detected in the plasma of rhesus macaques using a commercial ELISA assay carried out according to Dr. Siddappa Byrareddy and Dr. Aftab Ansari.

Cloning and characterization of rhesus macaque TIM-3

Total RNA was isolated and purified from rhesus PBMCs using an RNeasy Mini Kit (Qiagen) and samples were incubated with RNase-free DNase I (Promega) at 37°C for 30 minutes to avoid amplification of contaminating genomic DNA. First strand cDNA was

reverse transcribed from the total RNA with the Enhanced Avian First Strand Synthesis Kit (Sigma) using oligo$(dT)_{23}$ primers. PCR amplifications of first strand cDNA were carried out using the sense primer pTIM-3 and anti-sense primer pTIM-3-R (Fig. 9). Primers were designed using BLAST (NCBI) for human cDNA with the rhesus genome. The amplified fragments were ligated via T/A overhangs into the pGEM-T vector (Promega). The ligated plasmids were transformed and amplified in JM109 cells (Promega). The plasmids were purified and sequenced.

Construction of Fc fusion expression plasmid vectors

To construct the Fc fusion expression plasmids of extracellular TIM-3 corresponding to both IgV and mucin as well as its individual splice variants IgV and mucin, two pGEM-T vectors served as templates where each either carried full-length TIM-3 or rhesus IgG2 Fc (consisting of the hinge region, CH2 and CH3 domains). Two amino acid substitutions were introduced into the Fc domain to eliminate potential interactions with Fc receptors and complement, L235A and P331S, respectively. Extracellular TIM-3 was PCR amplified out using sense primer pTIM-3 (NcoI) and anti-sense primer pMucin-R (Fc). Anti-sense primer pMucin-R (Fc) contains the first 20 nt complement to IgG2 Fc. The IgG2 Fc encoding fragment was PCR amplified out using sense primer PAmigg2b and anti-sense primer IgG6ae (EcoRI). With a common 20 nt sequence, these two fragments were than joined by overlapping PCR using sense primer pTIM-3 (NcoI) and anti-sense primer pMucin-R (Fc). The resulting product was digested with *NcoI* and *EcoRI* and ligated into the pMT vector (Life Technologies) previously digested with *NcoI* and *EcoRI*, resulting in pMT TIM-3-Fc. The IgV domain was PCR amplified out using sense primer pTIM-3 (NcoI) and anti-sense

primer pIgV-R (Fc) while the mucin domain was PCR amplified out using sense primer pMucin (NcoI) and anti-sense primer pMucin-R (Fc). The same strategy used to fuse extracellular TIM-3 to IgG2 Fc was applied to the IgV domain and mucin domain, resulting in pMT IgV-Fc and pMT mucin-Fc, respectively.

Cell transfection

Drosophila Schneider 2 (S2) cells were grown in S2 medium (Life Technologies) containing 10% heat-inactivated fetal bovine serum, 5 U/ml penicillin and 5 μg/ml streptomycin at 27°C in an incubator to a density of 10 – 20 x 10^6 cells/mL. While in log phase growth, S2 cells were co-transfected by electroporation with either pMT TIM-3-Fc, pMT IgV-Fc or pMT mucin-Fc, with pCoHygro vector expressing the resistance gene to hygromycin at a 15:1 ratio using Nucleofector Solution and the Nucleofector Device (Lonza). Three days after transfection, the cells were selected in culture medium containing 300 μg/mL of hygromycin (Invivogen). After selection, the transfected S2 cells were expanded to a density of 30 – 40 x 10^7 cells/mL and protein production induced with 500 μM $CuSO_4$. Supernatants were harvested over 7 days and Fc fusion proteins purified by affinity chromatography with Protein G sepharose (Life Technologies). The column was washed and Fc fusion protein was eluted using acetate buffer (pH 2.6). The elution was neutralized immediately, and dialyzed against phosphate-buffered saline (PBS). Protein concentrations were quantified by the Pierce BCA Protein Assay Kit (Life Technologies) and subsequently lyophilized and stored at 4°C with desiccant.

SDS-PAGE and Western Analysis

Fc fusion proteins were boiled in SDS-PAGE sample buffer with or without 2-mercaptoethanol for 5 minutes. The samples (4 μg protein per well) were separated on 10% Tris glycine SDS-PAGE (Lonza) along with bovine serum albumin (BSA) and the Precision Plus Protein Dual Color Standard (Bio-Rad) markers. For SDS-PAGE analysis, the proteins were detected by staining with Bio-Safe Coomassie (Bio-Rad). For Western blot analysis, the gels were electrotransferred to nitrocellulose membranes. The membranes were blocked with 5% BSA in PBST (0.05% Tween 20 in PBS) for 1 hour, and alkaline-phosphatase-conjugated rabbit anti-monkey IgG (Sigma) (raised against monkey Fc) was added at a dilution of 1:1000 to 1% BSA in PBST for 1 hour. The membrane was washed with PBS and developed with alkaline phosphatase substrate. Western analysis was repeated using goat anti-TIM-3 polyclonal antibody (R&D Systems) as the primary antibody followed by anti-goat IgG as the secondary antibody.

Galectin-9 binding assays

Maxisorp ELISA plates were coated 24 hours before the assay using 0.2 μg of recombinant human galectin-9 (R&D Systems) or BSA in a volume of 100 μL of 1X coating buffer. Serial dilutions of TIM-3-Fc, IgV-Fc, and mucin-Fc were added and incubated for 1 hour at 37°C. The plate was washed and blocked with 1% BSA in PBST incubated for 1 hour at 37°C. The plate was washed and horseradish peroxidase-conjugated anti-human IgG was added at a dilution of 1:1000 to 1% BSA in PBST for 1 hour at 37°C. TMB Peroxidase Substrate (KPL) was added and developed prior to stopping the reaction with 2N H_2SO_4. Absorbance was measured at 490 nm.

Staining for TIM-3 ligand

Purified TIM-3-Fc was chemically conjugated to R-PE (ab102918, Abcam) according to manufacturer protocol. Isolated PBMCs were then incubated with various amounts of Tim3-Fc/R-PE in the absence or presence of 10% rhesus heparin plasma to inhibit non-specific binding along with the antibody cocktail mix against CD3, CD20, NKG2A, HLADR, CD14, CD16, and CD11c for 30 minutes at 4°C in the dark. Then, PBMCs were washed with FACS solution, fixed in 1% PFA, and acquired on BD LSRII flow cytometer (BD Biosciences).

Proliferation assay

Briefly, 1 x 10^7 PBMCs were labeled with 3 μM carboxyfluorescein diacetate succinimidyl ester (CFSE) and washed with ice-cold RPMI-1640 medium containing 10% FBS, 100 units/ml penicillin/streptomycin and 2mM L-glutamine (complete medium). The CFSE-labeled cells were adjusted to 1 – 2 x 10^6 cells/0.6 ml, transferred to a 48-well plate, and stimulated with or without a mixture of SIV gag peptides covering the entire SIV gag sequence (20-mers overlapping by 12) (2 μg/ml) in the presence or absence of TIM-3-Fc (10 μg/ml), PD-1-Fc (5 μg/ml), or anti-PD-1 monoclonal antibody (10 μg/ml) at 37°C, 7% CO_2. After 6 days of incubation cells were harvested and stained for specific markers. The cells were washed with FACS solution and stained with Live/Dead marker (Alexa 430, Invitrogen A10169) at room temperature for 30 minutes and washed with complete medium. Labeled cells were then stained with the antibody cocktail containing Alexa Fluor 700-conjugated anti-CD3 (clone SP34-2, BD), peridinin-chlorophyll protein-conjugated anti-CD4 (clone L200, BD) and BD Horizon V450-conjugated anti-CD8 (clone RPA-T8, BD).

After incubation for 30 minutes at 4°C, PBMCs were washed with FACS solution, fixed in 1% PFA, and acquired on a LSRII flow cytometer (BD Biosciences) driven by the FACS DiVa software. Analysis of the acquired data was performed using FlowJo software (version 9.2; TreeStar, Ashland, OR).

Results

Expression of TIM-3 on different cells in humans and rhesus macaques

In order to explore the role of TIM-3 in the rhesus macaque model of AIDS, we evaluated the expression of Tim-3 on PBMCs from uninfected rhesus macaques and healthy human donors. As shown in Fig. 4, there are significant differences in the TIM-3 expression profile of PBMCs from the two species. The frequencies of TIM-3-expressing cells were markedly lower for $CD4^+$, $CD8^+$ T cells, $NKG2A^+$ natural killer (NK) cells, mDCs, and plasmacytoid dendritic cells (pDCs) from rhesus macaques compared to humans (Fig. 4). In contrast, the frequency of TIM-3-expressing $CD20^+$ B cells from rhesus macaques was markedly higher than from humans. However, TIM-3 expression on rhesus macaque T cells has been documented to increase early after SIV infection (30).

TIM-3 and PD-L2 are expressed by different subsets of mDCs

We next investigated the expression of TIM-3 and PD-L2 on dendritic cells in PBMCs, as interaction of TIM-3 with galectin-9 (36) and PD-L2 with PD-1 (37) has been suggested to lead to T cell activation and inhibition respectively. Interestingly, analysis of mDCs subpopulations revealed a clear separation between $TIM\text{-}3^+$ and $PD\text{-}L2^+$ mDCs (Fig. 5A).

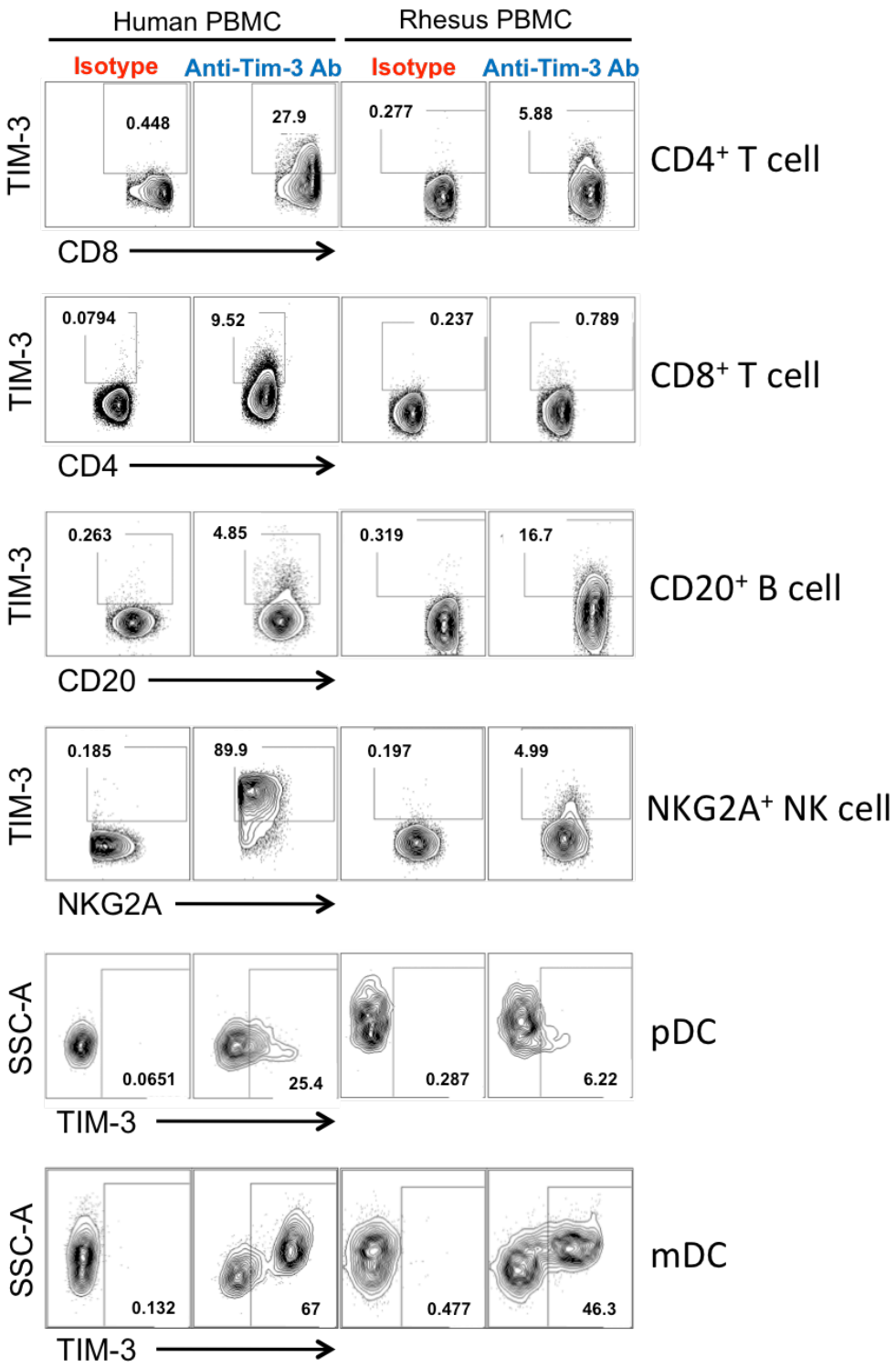

Figure 4. Expression of TIM-3 on the various immune cell populations. Flow plots depict TIM-3 expression on CD4+ T cells, CD8+ T cells, CD20+ B cells, NKG2A+ NK cells, CD11c+ mDCs, and CD123+ pDCs from PBMCs in representative humans or rhesus macaques.

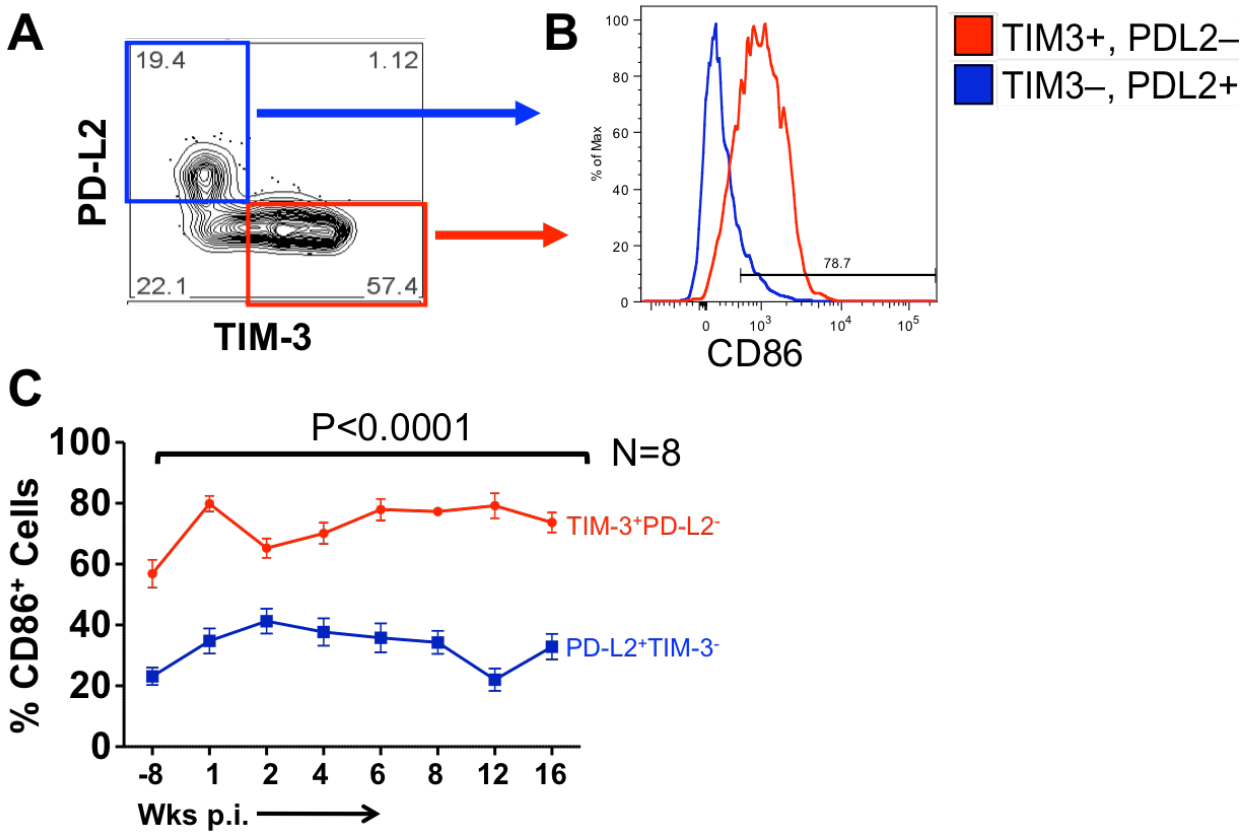

Figure 5. Expression of CD86 on TIM-3⁺ mDCs pre-infection and post-infection. **(A)** Flow cytometric analysis of naïve rhesus macaque mDCs based on PD-L2 and TIM-3 expression. **(B)** Expression of CD86 on mDCs gating on TIM-3⁺PD-L2⁻ and TIM-3⁻PD-L2⁺ mDCs. **(C)** Longitudinal analysis of CD86 expression on mDCs gating on TIM-3⁺PD-L2⁻ and TIM-3⁻PD-L2⁺ mDCs.

TIM-3 expressing mDCs show a more activated phenotype

Maturation states for DCs have been defined with the "immature state" characterized by low levels of antigen-presenting MHC-I and MHC-II gene products (38) as well as co-stimulatory molecules such as CD86 (39), whereas the "mature state" is characterized by the converse. Of note, immature DCs tend to induce tolerance whereas mature DCs elicit antigen-specific effector functions. We analyzed the two unique mDC populations and showed that TIM-3⁺PD-L2⁻ mDCs express higher frequencies of CD86

compared to TIM-3⁻PD-L2⁺ mDCs (Fig. 5B). Longitudinal monitoring of CD86 expression of the two populations showed the TIM-3⁺PD-L2⁻ population peaks at 1 week post-infection, followed by a transient decrease at 2 weeks post-infection, and an overall increased frequency at 16 weeks post-infection compared to pre-infection (Fig. 5C). In contrast, the TIM-3⁻PD-L2⁺ population suspected to be inducing T cell activation had a transient increase at 4 weeks post-infection, followed by a decrease at 12 weeks post-infection, and over an overall increased frequency at 16 weeks post-infection compared to pre-infection.

TIM-3⁺ mDCs respond to TLR3 agonist

An increased frequency of activated mDCs over time suggested mDC recognition of viral components, such as protein or dsRNA, through the Toll-like receptors (TLRs). We then asked whether the distinct mDC populations would respond to dsRNA in a TLR-3-dependent manner, triggering the release of inflammatory cytokines such as tumor necrosis factor alpha (TNF-α) and IL-12. We also included lipopolysaccharide as a TLR-4 agonist for a control. As shown in Fig. 5, the TLR-4 agonist induced robust expression of TNF-α and IL-12 in TIM-3⁻PD-L2⁺ mDCs, while the TLR-3 agonist did not induce a measurable response. We also note stimulation of TIM-3⁻PD-L2⁻ mDCs with TLR-4 agonist resulted in a similar, albeit weaker response while TLR-3 agonist induced mild expression of TNF-α (data not shown). Surprisingly, TIM-3⁺ PD-L2⁻ mDCs responded to the TLR-3 agonist, but not TLR-4 agonist, with increased TNF-α expression but with little IL-12 expression (Fig. 6A, 6B). Taken together, these data suggest TIM-3 as a marker for an mDC population able to respond to viral dsRNA, promoting inflammation rather than Th1 induction to lead to more potent CD4 and CD8 T cell responses.

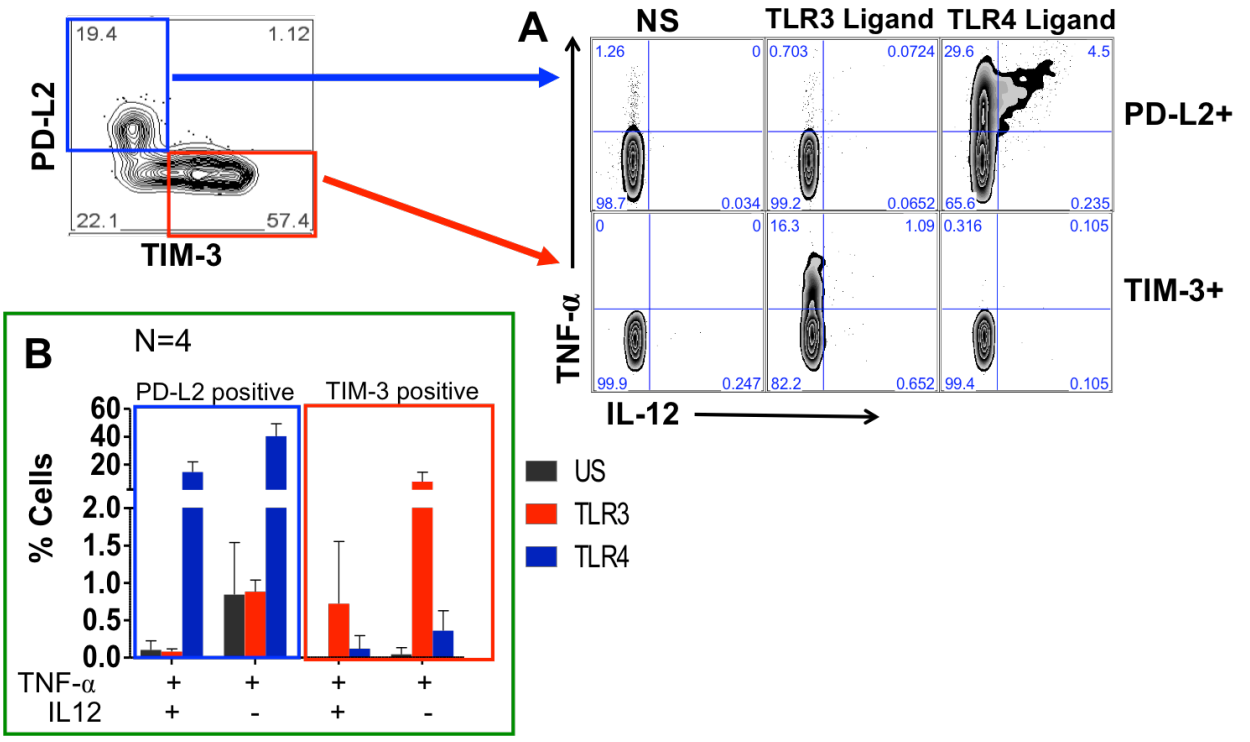

Figure 6. TLR agonist stimulation of the mDC populations. (A) Flow cytometric analysis of TNF-α and IL-12 secretion by TIM-3⁺ PD-L2⁻ and TIM-3⁻PD-L2⁺ mDCs under no stimulation, TLR-3 ligand (dsRNA) simulation, or TLR-4 ligand (lipopolysaccharide) stimulation. **(B)** Quantitative analysis of TNF-α and IL-12 secretion by TIM-3⁺PD-L2⁻ and TIM-3⁻PD-L2⁺ mDCs under no stimulation, TLR-3 ligand (dsRNA) simulation, or TLR-4 ligand (lipopolysaccharide) stimulation.

High levels of soluble galectin-9 in SIV-infected rhesus macaques

Previous reports have examined galectin-9 as a ligand to TIM-3 (18, 40). To further elucidate potential mechanisms of TIM-3/galectin-9 interactions and immune responses, we examined plasma concentrations of galectin-9 in naïve and SIV-infected rhesus macaques. Plasma levels of galectin-9 were more than 15-times higher in the chronic phase of SIV infection relative to uninfected rhesus macaques (Fig. 7A). Among SIV-infected rhesus macaques, we distinguished elite controllers with delayed disease progression from non-controllers who developed clinical AIDS within 18 months post infection. Non-

controllers had significantly elevated levels of circulating galectin-9 compared to elite-controllers and naïve rhesus macaques (Fig. 7B). Longitudinal analysis of chronically SIV-infected non-controllers revealed a spike in galectin-9 at 2 weeks post-infection, which leveled out at 4 weeks post-infection and remained constant at least until 60 weeks post-infection (Fig. 7C). A similar pattern was observed for SIV-infected elite-controllers though at significantly lower levels of galectin-9, suggesting that galectin-9 may represent a correlate of disease progression and be involved in SIV disease pathogenesis.

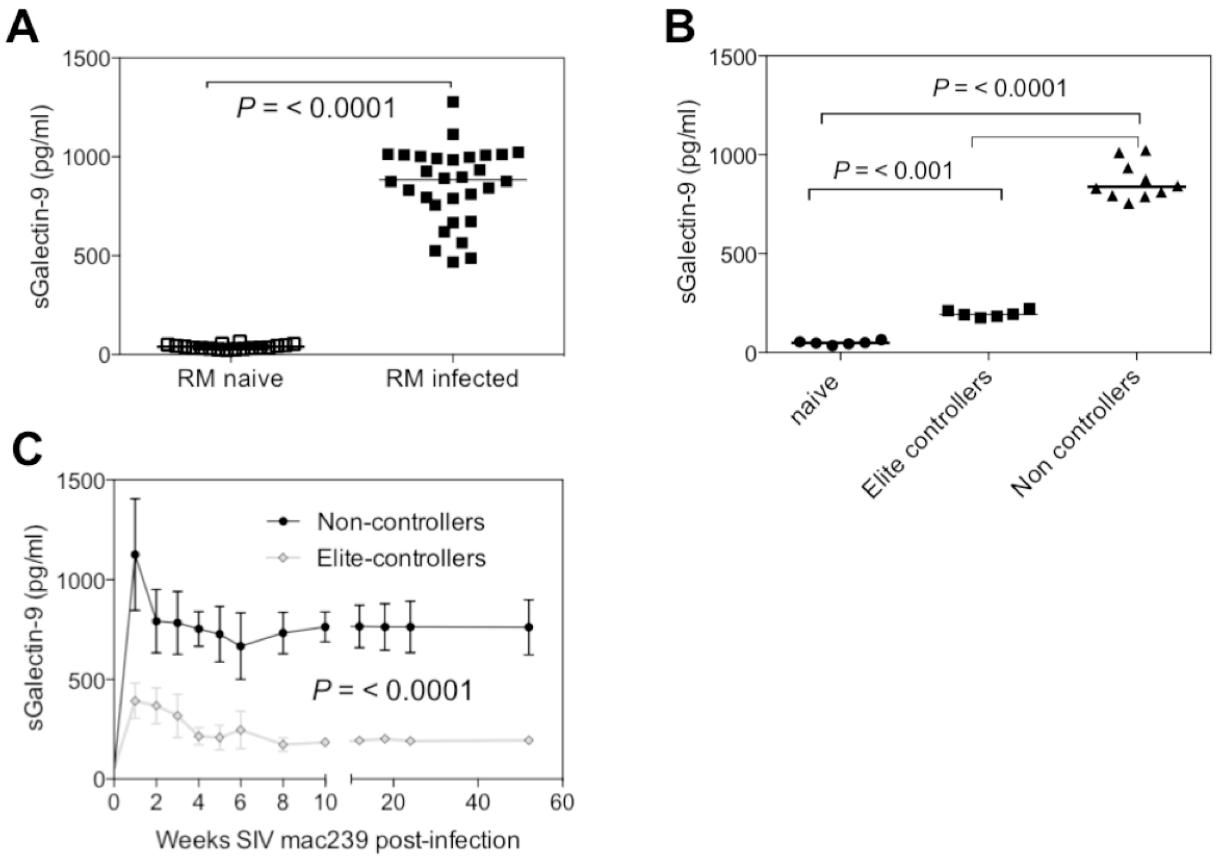

Figure 7. Plasma levels of soluble galectin-9 in naïve and SIV-infected rhesus macaques. (A) Dot plot represents the concentration of soluble galectin-9 (sGalectin-9) in the plasma of 30 rhesus macaques pre- and post-infection as determined by ELISA. **(B)** Dot plot represents the concentration of soluble galectin-9 in the plasma of naïve rhesus macaques, SIV-infected elite controllers, and SIV-infected non-controllers. **(C)** Longitudinal

analysis of the concentration of soluble galectin-9 in elite controllers and non-controllers post-SIV infection.

Various cell populations express intracellular galectin-9

In order to determine the predominant producer of galectin-9, we assessed intracellular levels in different immune cells by flow cytometry. Staining revealed high levels of intracellular galectin-9 in CD3⁺ T cells, CD20⁺ B cells, NKG2A⁺ NK cells, CD14⁺CD16⁻ and CD16⁺CD14⁻ monocytes, and CD11c⁺ mDCs (Fig. 8).

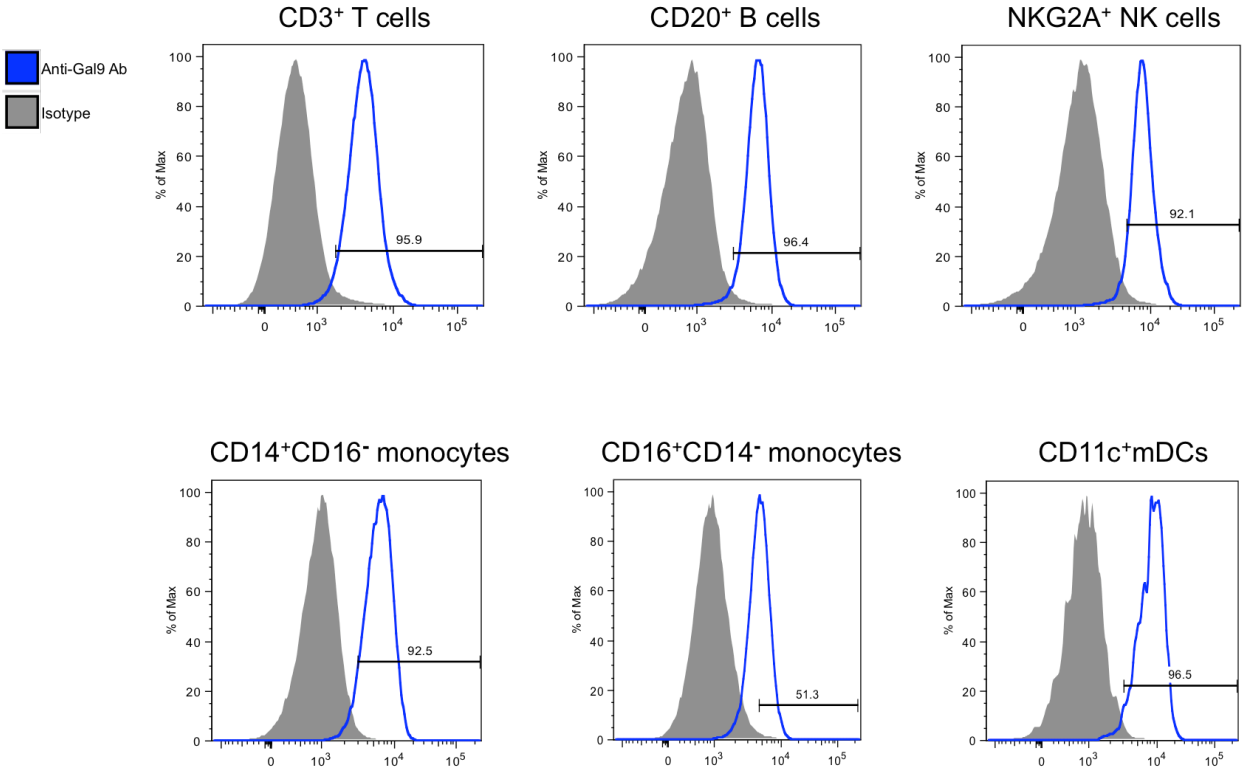

Figure 8. Intracellular staining of various immune cell populations for galectin-9. Flow cytometry gating strategy to analyze intracellular expression of galectin-9 on CD3⁺ T cells, CD20⁺ B cells, NKG2A⁺ NK cells, CD14⁺CD16⁻ monocytes, CD16⁺CD14⁻ monocytes, and CD11c⁺ mDCs.

Cloning of TIM-3

In order to characterize rhesus TIM-3, we generated cDNA from RNA isolated from rhesus PBMCs (Fig. 9). The isolated cDNA shares a high similarity (90%) with human TIM-3, and the amino acid sequences also shows high homology (85%) with human TIM-3 protein (Fig. 10). Alignment of the amino acid sequence with the endogenous human and murine TIM-3 reveals a conservation of the domains, consisting of the signal peptide, IgV, mucin, transmembrane and cytoplasmic domains. Of interest, we noted a nine amino acid deletion in the mucin domain, appearing before the beginning of the transmembrane domain. The deletion in rhesus TIM-3 does not a priori have any detectable functional alteration due to its location within the mucin stalk.

Primer Name		Sequence (specified for 5' to 3')
Cloning Primers		
pTIM-3	S	TCAGAAGTGGAATACATAGCAG
pTIM-3-R	A	CTATGGCACTGCAACGCGACAA
Subcloning Primers		
pTIM-3 (**NcoI**)	S	TATA / **CCATGG** / TCAGAAGTGGAATACATAGCAG
pIgV-R (*Fc*)	A	*GGTGGGCACGTAGATCTACC* / TGGTTTGATGACGACCAACTTC
pMucin (**NcoI**)	S	CC / **CCATGG** / GCCAAGGTCACCCCTGCACCAA
pMucin-R (*Fc*)	A	*GGTGGGCACGTAGATCTACC* / TCTGATGGTTGCTCCAGAGTC
PAmigg2b	S	GGTAGATCTACGTGCCCACCGTGCCCAGCTGAA
IgG6ae (**EcoRI**)	A	TATGACGTC / **GAATTC** / TCATTTACCCGGAGACACGGAGA

Figure 9. Primer list for cloning and subcloning TIM-3. "Primer Name" column indicates the use of restriction digest sites in bold and the use of a 20 nt sequence corresponding to IgG2 Fc for overlapping PCR application in italics. "S" refers to sense primer, while "A" refers to anti-sense primer.

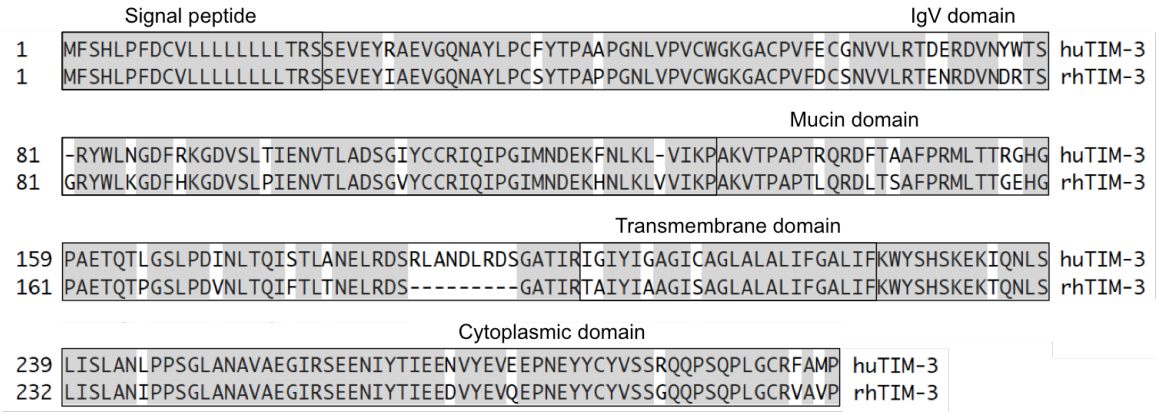

Figure 10. Alignment of the amino acid sequences of human TIM-3 (huTIM-3) and rhesus TIM-3 (rhTIM-3). Highlighted sequences indicate homology between endogenous human and rhesus TIM-3. Dashes indicate gaps in alignment.

Construction of TIM-3-Fc fusion proteins

To explore the function of extracellular TIM-3 as well as its domains, we subcloned the IgV and mucin domains. For downstream applications, recombinant proteins can prove challenging with purification and their use in vivo may be limited by their relatively short half-life. We addressed these issues by using overlapping PCR to fuse rhesus IgG2 Fc to extracellular TIM-3, IgV domain, or mucin domain to generate TIM-3-Fc, IgV-Fc, and mucin-Fc (Fig. 11, 12). It is important to note two amino acid mutations were made in IgG2 Fc (L235A and P331S) to eliminate potential binding of C3 for complement activation and Fc receptors for antibody-dependent cellular cytotoxicity (ADCC), but still retain recycling via the FcRn salvage pathway (41). This approach of fusing IgG2 Fc to TIM-3 is expected to (1) increase the circulating half-life of TIM-3 since TIM-3-Fc will be secreted as a homodimer with a higher molecular weight and thus be in circulation longer due to not being filtered out by the kidneys; (2) enhance TIM-3 binding of TIM-3 ligands by the homodimers; and (3) facilitate purification of TIM-3-Fc through the use of Protein G Sepharose.

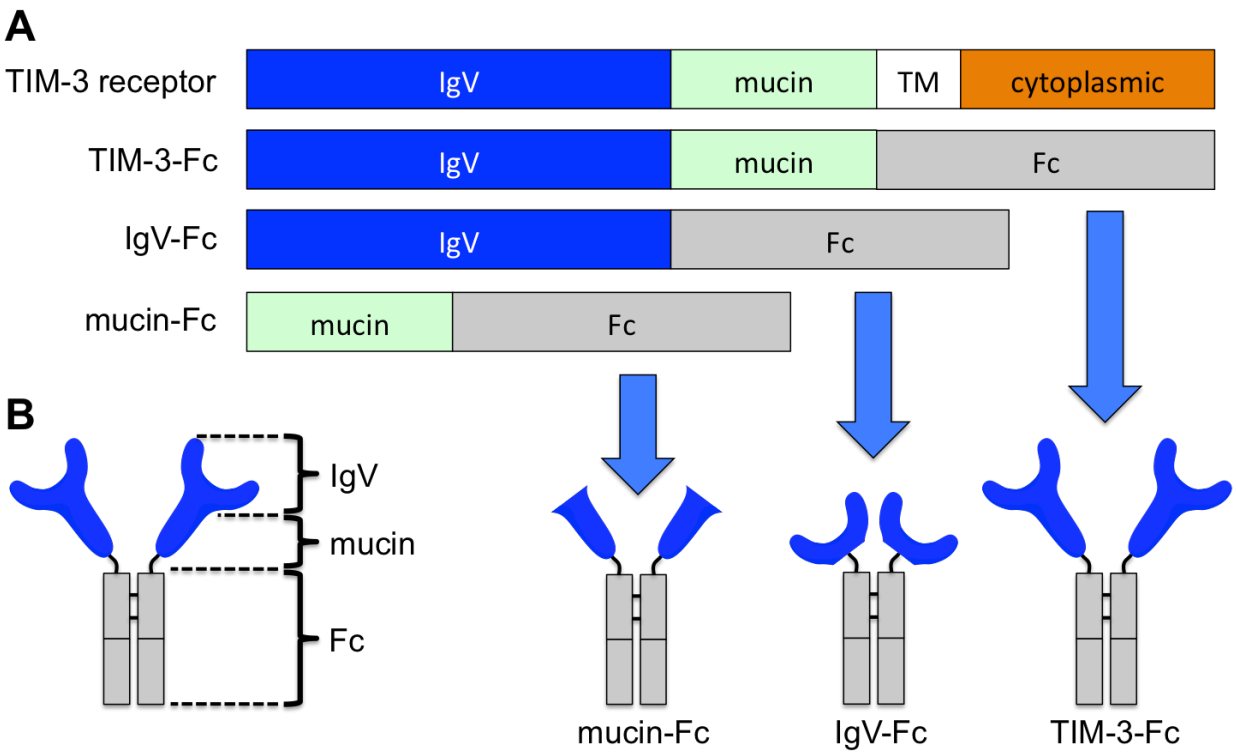

Figure 11. Construction of TIM-3 and its splice variants as Fc fusion proteins. (A) The genes encoding for endogenous TIM-3, full-length TIM-3 fused to Fc domain, TIM-3 IgV fused to Fc domain, and TIM-3 mucin fused to Fc domain. **(B)** The individual domains of the full-length TIM-3-Fc fusion protein.

Key: IgV domain (red), mucin domain (green), and antibody hinge and Fc regions (blue).

TIM-3-Fc IgV domain; Mucin domain; IgG2 hinge and Fc

SEVEYIAEVGQNAYLLCSYTPAPPGNLVPVCWGKGACPVFDCSNVVLRTENRDVNDRTSGRYWLK
GDFHKGDVSLTIENVTLADSGVYCCRIQIPGIMNDEKHNLKLVVIKPAKVTPAPTLQRDLTSAFPR
MLTTGEHGPAETQTPGSLPDVNLTRIFTLTNELRDSGATIRGRSTCPPCPAELAGGPSVFLFPPKPK
DTLMISRTPEVTCVVVDVSQEEPDVKFNWYVDGVEVHNAQTKPREEQFNSTYRVVSVLTVTHQD
WLNGKEYTCKVSNKGLPASRQKTVSKTKGQPREPQVYTLPPPREELTKNQVSLTCLIKGFYPSDIV
VEWASNGQPENTYKTTPPVLDSDGSYFLYSKLTVDKSRWQQGNVFSCSVMHEALHNHYTQKSLS
VSPGK

IgV-Fc IgV domain; IgG2 hinge and Fc

SEVEYIAEVGQNAYLLCSYTPAPPGNLVPVCWGKGACPVFDCSNVVLRTENRDVNDRTSGRYWLK
GDFHKGDVSLTIENVTLADSGVYCCRIQIPGIMNDEKHNLKLVVIKPGRSTCPPCPAELAGGPSVFL
FPPKPKDTLMISRTPEVTCVVVDVSQEEPDVKFNWYVDGVEVHNAQTKPREEQFNSTYRVVSVL
TVTHQDWLNGKEYTCKVSNKGLPASRQKTVSKTKGQPREPQVYTLPPPREELTKNQVSLTCLIKG
FYPSDIVVEWASNGQPENTYKTTPPVLDSDGSYFLYSKLTVDKSRWQQGNVFSCSVMHEALHNH
YTQKSLSVSPGK

mucin-Fc Mucin domain; IgG2 hinge and Fc

AKVTPAPTLQRDLTSAFPRMLTTGEHGPAETQTPGSLPDVNLTRIFTLTNELRDSGATIRGRSTCP
PCPAELAGGPSVFLFPPKPKDTLMISRTPEVTCVVVDVSQEEPDVKFNWYVDGVEVHNAQTKPRE
EQFNSTYRVVSVLTVTHQDWLNGKEYTCKVSNKGLPASRQKTVSKTKGQPREPQVYTLPPPREEL
TKNQVSLTCLIKGFYPSDIVVEWASNGQPENTYKTTPPVLDSDGSYFLYSKLTVDKSRWQQGNVF
SCSVMHEALHNHYTQKSLSVSPGK

Figure 12. Sequences of TIM-3-Fc, IgV-Fc and Mucin-Fc. The amino acid sequences of TIM-3-Fc, IgV-Fc, and Mucin-Fc are shown. The IgV domains are indicated in red, Mucin domains are indicated in green, and Fc domains are indicated in blue.

In addition, we used S2 insect cells for the expression and production of the TIM-3-Fc fusion proteins (Fig. 13). Compared to the mammalian cell culture approach, S2 insect cells carry the advantages of quick and easy transfection, ease of handling, and ability to stably scale up for high titers. Prior repeated use of recombinant macaque proteins produced in S2 insect cells in vivo has shown good tolerability and an absence of immune recognition, suggesting that the proteins produced in this system are folded correctly, even though differences in glycosylation exists relative to mammalian cell produced proteins. These differences have not been shown to affect secondary functions such as complement activation and ADCC (42).

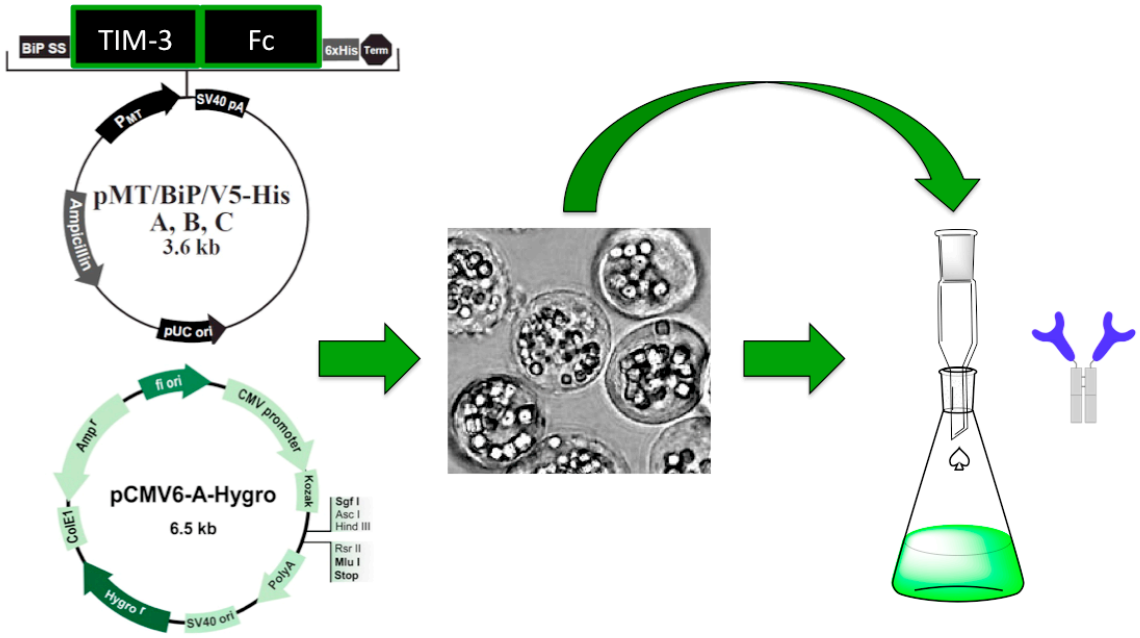

Figure 13. Expression of TIM-3-Fc in S2 insect cells. Schematic outline of the TIM-3-Fc production process beginning with subcloning the TIM-3-Fc gene into the pMT vector, followed by co-transfection with the pCoHygro vector into S2 insect cells. After induction, supernatant is collected and filtered through a Protein G Sepharose column to purify and isolate the TIM-3-Fc protein.

To confirm the successful transfection of S2 insect cells, an aliquot of transfected insect cells was lysed for amplification of the transfected plasmids using gene-specific primers (Fig. 9). The supernatants from the transfected insect cells were also examined for the presence of the Fc fusion proteins by Coomasie Blue staining of the SDS-PAGE gel (Fig. 14A) and Western blot using HRP-conjugated anti-IgG2 Fc antibodies (Fig. 14B) as well as with polyclonal anti-TIM-3 antibody (data not shown). SDS-PAGE and Western blot detected a 50 kDa and 100 kDa bands for TIM-3-Fc under reducing and non-reducing conditions, respectively; a 44 kDa and 88 kDa band for IgV-Fc under reducing and non-reducing conditions, respectively; and a 37 kDa and 74 kDa band for mucin-Fc under reducing and non-reducing conditions, respectively. These findings confirm the secretion of the Fc fusion proteins by transfected insect cells and the homodimerized TIM-3-Fc fusion proteins exist in native conditions.

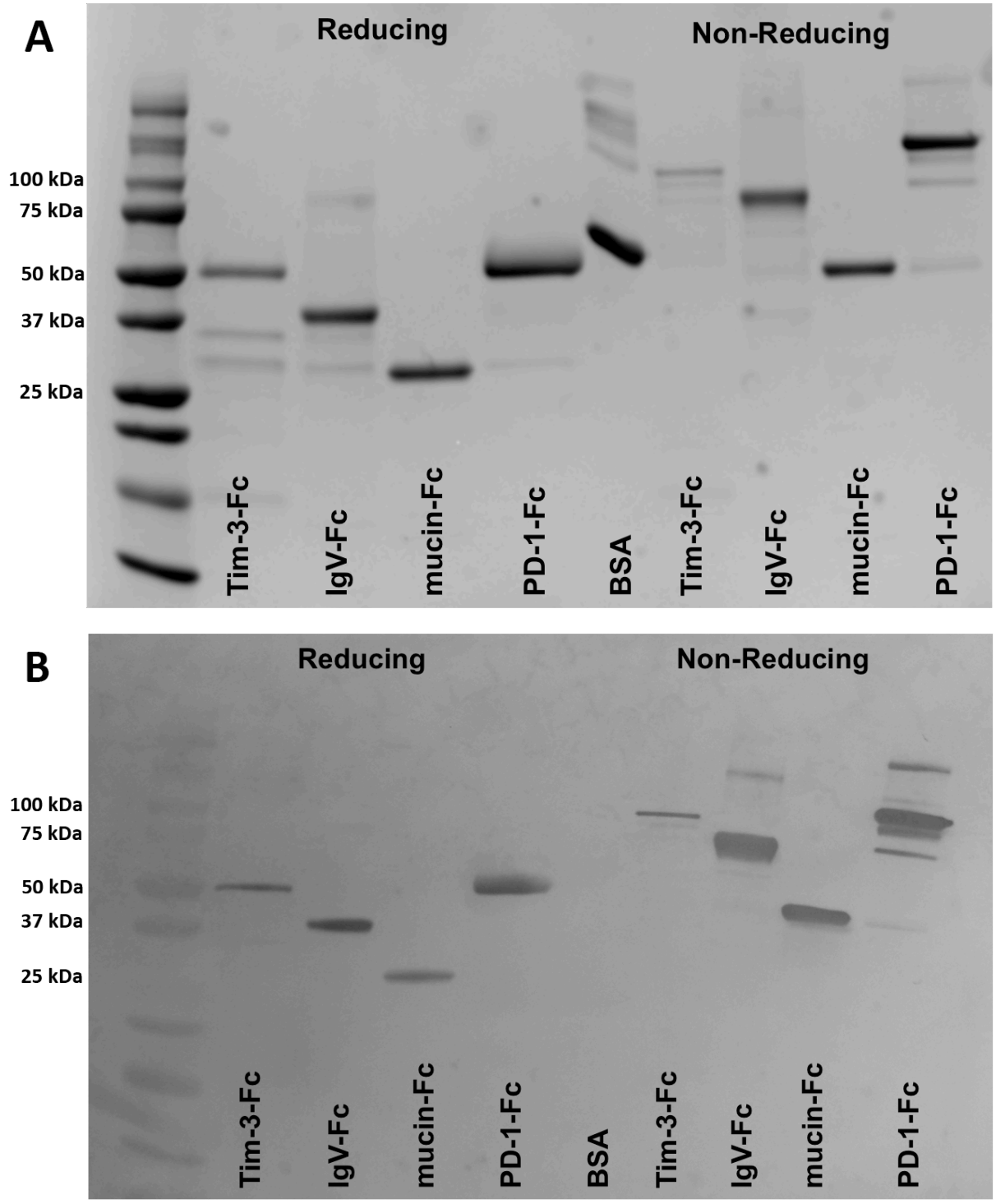

Figure 14. SDS-PAGE and Western blot analysis of the various Fc fusion proteins. **(**A) SDS-PAGE and **(B)** Western analysis of TIM-3-Fc, IgV-Fc, and mucin-Fc along with PD-1-Fc and BSA as controls under reducing and non-reducing conditions. Western blot staining was for the Fc domain.

Binding of galectin-9 to the TIM-3 IgV domain but not the mucin domain

To evaluate whether the purified TIM-3-Fc fusion proteins were functional as well as establish whether galectin-9 was a ligand for TIM-3, we tested TIM-3-Fc, IgV-Fc, and mucin-Fc for their abilities to bind galectin-9 in an ELISA format. TIM-3-Fc and IgV-Fc showed similar binding kinetics to plate bound galectin-9 (Fig. 15). In contrast, the mucin-Fc did not show any significant binding to galectin-9. This suggests galectin-9 specifically recognizes and binds to the IgV domain of TIM-3.

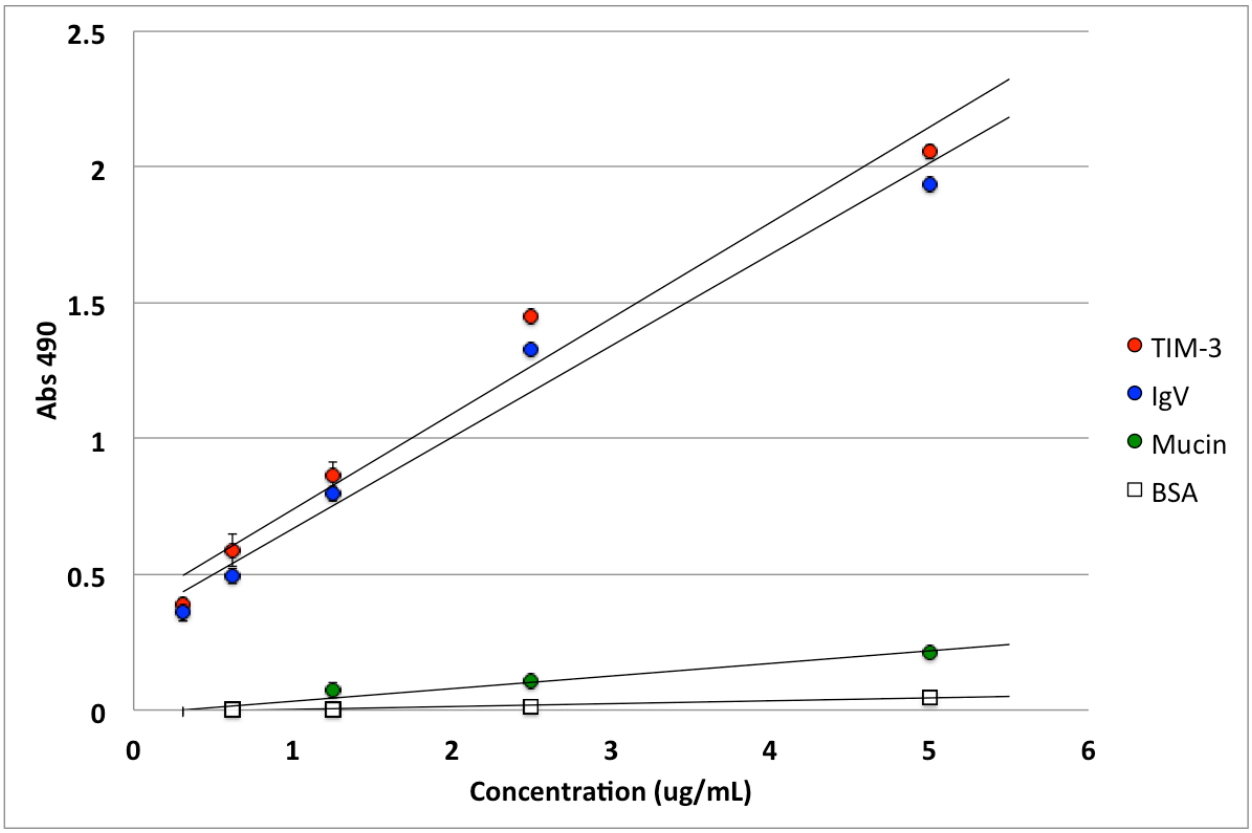

Figure 15. Binding activity of TIM-3-Fc, IgV-Fc, and mucin-Fc to immobilized galectin-9. Serial dilutions of the Fc fusion proteins were added to immobilized galectin-9 and detected by HRP-conjugated anti-IgG antibody. Binding activity was measured by fluorescence generated by substrate oxidation via HRP activity.

Expression of TIM-3 ligand

To explore TIM-3 ligand expression, we chemically conjugated R-PE to TIM-3-Fc and stained total PBMCs followed by normal gating strategy. We carried out TIM-3 ligand expression analysis in the absence and presence of 10% rhesus heparin plasma to minimize background by blocking potential FcRn interactions. Surprisingly, blocking with serum did not reduce but enhanced TIM-3-Fc binding to TIM-3 ligand, for reasons that need further investigation. TIM-3-Fc/R-PE bound to resting $CD14^{+}CD16^{-}$, $CD16^{+}CD14^{-}$, and $CD14^{+}CD16^{+}$ monocytes as well as on $CD20^{+}$ B cells and $CD11c^{+}$ mDCs, confirming the data generated with anti-galectin-9 staining (Fig. 8). We also observed binding on $CD4^{+}$ and $CD8^{+}$ T cells, though at markedly lower levels than B cells, monocytes, or mDCs (Fig. 16). All reported binding increased in a dose-dependent manner.

In vitro blockade of the inhibitory TIM-3 pathway with TIM-3-Fc

To study the effect of blocking the interaction between TIM-3 and its ligands during in vitro stimulation of SIV-antigen specific cells, we used our recombinant TIM-3-Fc. No monoclonal antibody raised against rhesus TIM-3 has been described or been characterized for blockade experiments. Instead, our benchmark was the targeted inhibition of the PD-1 pathway using either monoclonal antibody against PD-1 (34) or recombinant PD-1-Fc prepared as previously described (35). Both of these inhibitors of the PD-1 pathway have shown success in enhancing proliferation SIV-specific $CD4^{+}$ and $CD8^{+}$ T cells.

Thus, PBMCs from four chronically infected (150 weeks post-SIV infection, plasma viral loads as viral copies/mL are followed: RM1, undetermined; RM2, 242755; RM3,

undetermined; RM4, 5604) rhesus macaques were labeled with CFSE and stimulated for 6 days with a mixture of SIV gag peptides covering the entire SIV gag sequence in the presence or absence of TIM-3-Fc, PD-1-Fc, or anti-PD-1 monoclonal antibody. All $CD4^+$ and $CD8^+$ T cells proliferated when incubated with the pool of SIV gag peptides (data not shown). TIM-3-Fc by itself did not induce proliferation of either $CD4^+$ or $CD8^+$ T cells in the absence of SIV gag peptides (data not shown). As previously reported, we observed modest enhancement of proliferation of SIV gag-specific $CD4^+$ and/or $CD8^+$ T cells using PD-1-Fc or anti-PD-1 (Fig. 17), perhaps due to the timing of collection post SIV infection. For two rhesus macaques, the presence of TIM-3-Fc enhanced the proliferation of SIV-specific $CD4^+$ but not $CD8^+$ T cells (Fig. 17). Overall, the in vitro restoration of these responses seemed limited and variable from animal to animal, not only in the presence of TIM-3-Fc, but also with PD-1-Fc and anti-PD-1, which may be secondary to the late collection time point post SIV infection. Testing of additional animals and time points are ongoing.

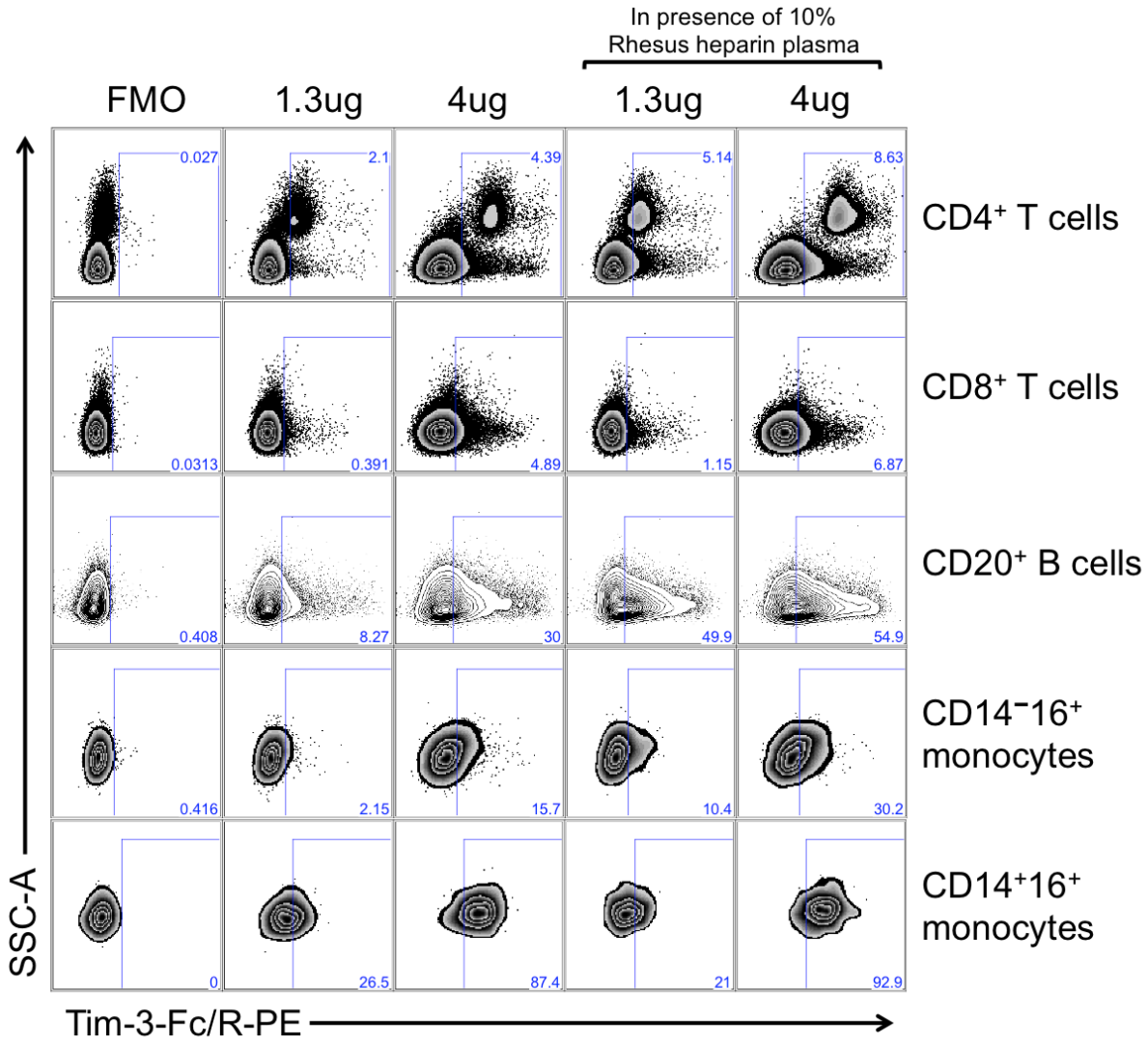
In presence of 10%
Rhesus heparin plasma
FMO
1.3ug
4ug
1.3ug
4ug
0.027
2.1
4.39
5.14
8.63
CD4+ T cells
0.0313
0.391
4.89
1.15
6.87
CD8+ T cells
0.408
8.27
30
49.9
54.9
CD20+ B cells
0.416
2.15
15.7
10.4
30.2
CD14-16+ monocytes
0
26.5
87.4
21
92.9
CD14+16+ monocytes
SSC-A
Tim-3-Fc/R-PE

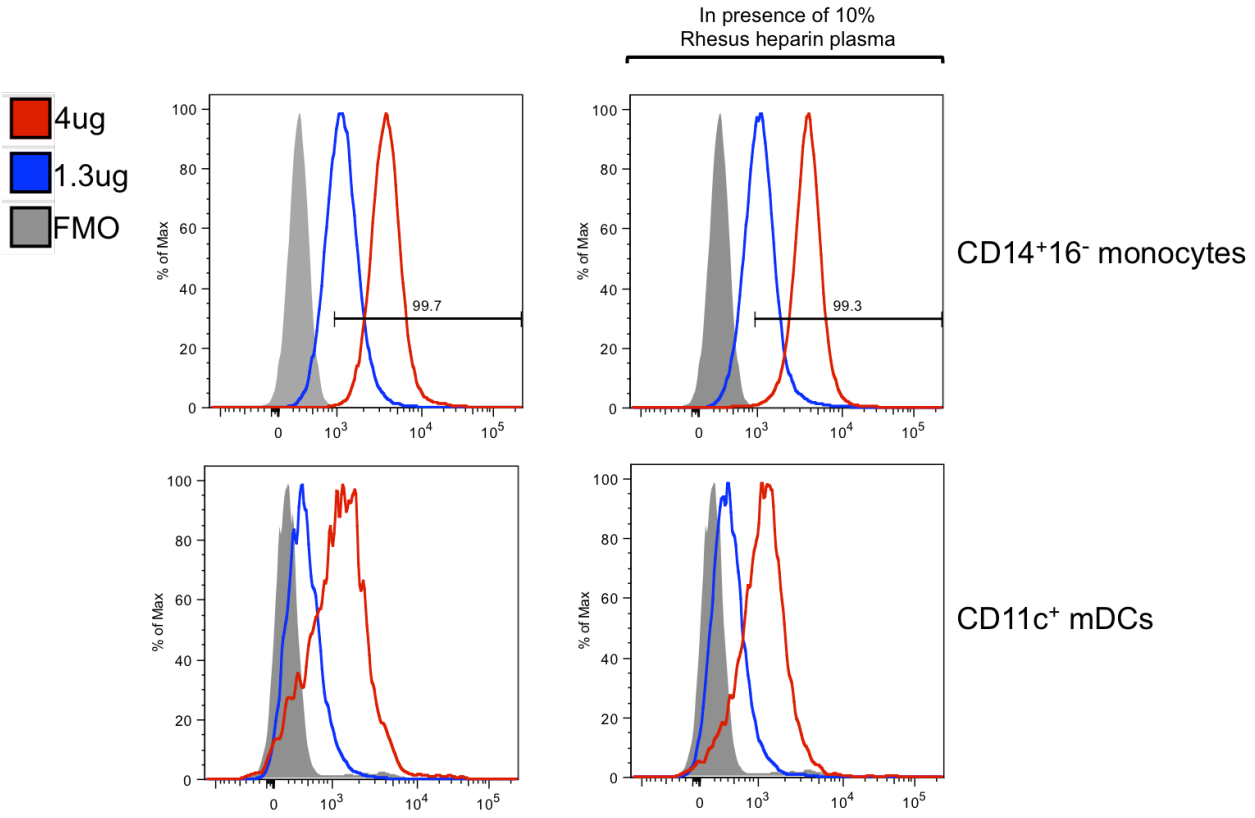

Figure 16. Staining for TIM-3 ligand on various immune cell populations using TIM-3-Fc/R-PE. Binding of TIM-3-Fc to TIM-3 ligand on CD4+ T cells, CD8+ T cells, CD20+ B cells, monocytes, and mDCs.

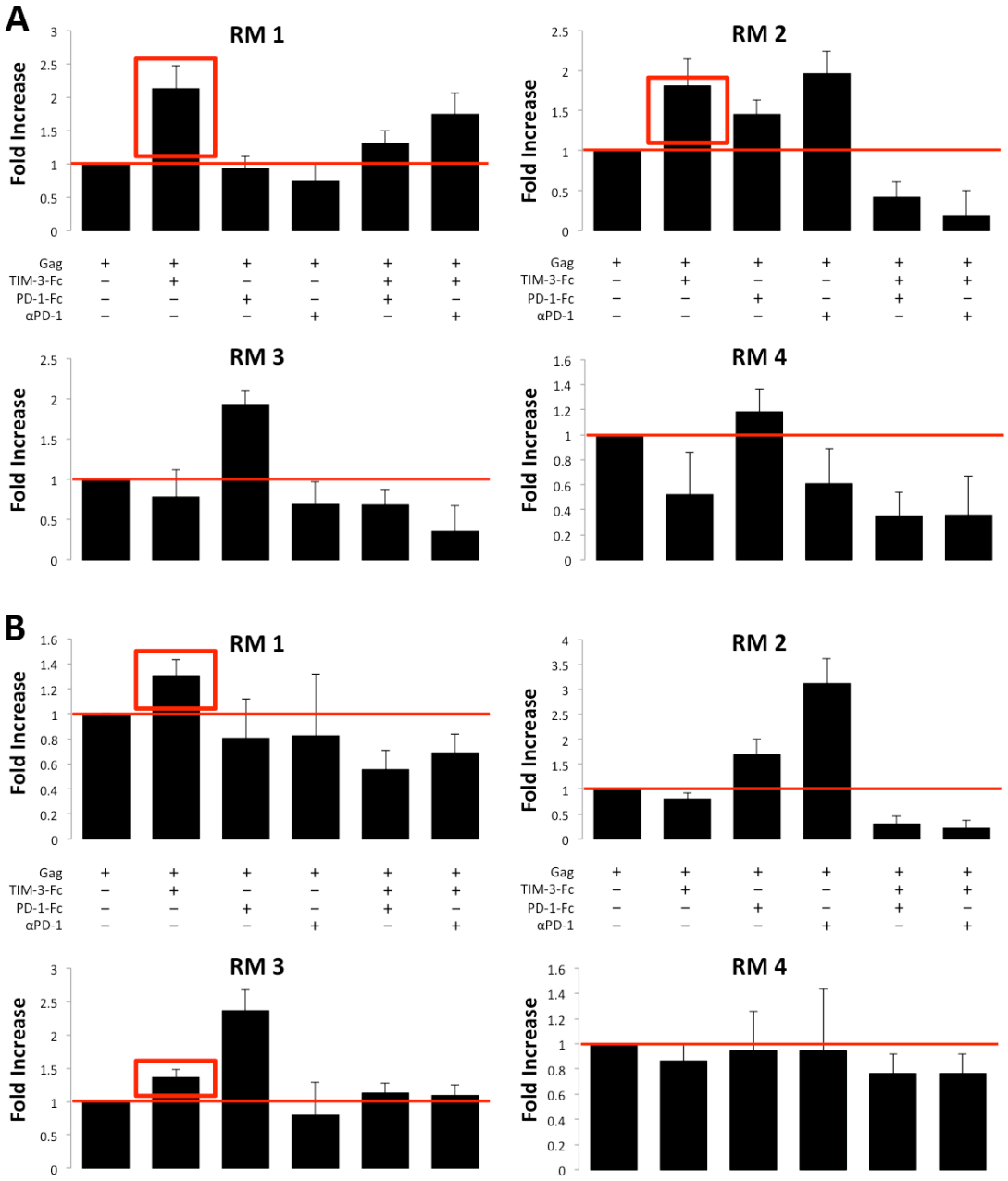

Figure 17. Proliferation of CD4⁺ and CD8⁺ T cells in response to in vitro blockade and SIV gag peptide stimulation. In vitro proliferative response of CSFE-labeled SIV gag-specific CD4⁺ **(A)** or CD8⁺ **(B)** T cells to a pool of overlapping SIV gag peptides in the absence (Gag) or presence of TIM-3-Fc (Gag + TIM-3-Fc), PD-1-Fc (Gag + PD-1-Fc), αPD-1 (Gag + αPD-1), as well as combinations using Fc fusions only (Gag + TIM-3-Fc + PD-1-Fc) or with antibody (Gag + TIM-3-Fc + αPD-1). The red line establishes the baseline fold increase in $CSFE^{Low}$ T cells where the SIV gag stimulated T cell population serves as the control. The red box highlights significant proliferative response of T cells in the presence TIM-3-Fc (Gag + TIM-3-Fc).

Discussion

Immune exhaustion represents a common phenomenon in many chronic diseases and cancer (43) as characterized by the loss of cytokine secretion, proliferation, and cytotoxicity in T cells. Immunological dialogue between activation and inhibitory signaling directs T cell activity, and strong inhibitory signaling facilitates functional impairment of antigen-specific T cells. PD-1 was among the first inhibitory receptors to be associated with immune exhaustion during chronic viral infection (8). It was previously thought immune exhaustion was irreversible, but remarkably, the in vivo blockade of PD-1 resulted in reduction of viral loads and recovery of virus-specific T cell activity and proliferation (34, 35). However, targeting the PD-1 pathway alone does not completely restore T cell function, suggesting additional inhibitory pathways remain to be elucidated.

TIM-3 was originally defined as a receptor involved in peripheral tolerance (16, 17), but has since expanded to include negative regulator of immunity after identifying upregulation of TIM-3 expression on dysfunctional HIV-specific T cells (12). Blockade of TIM-3 also results in enhanced T cell function and proliferation. However, studies of TIM-3 focus primarily on T cells, and the role of TIM-3 on other immune cell lineages remains largely unclear.

In this study, our goals were two-fold in that we wanted to characterize TIM-3 expression on T cells and on innate immune cell populations in rhesus macaques as well as explore the benefits of blocking the TIM-3 pathway. First, the expression of TIM-3 was found to markedly differ on primary immune cell lineages from humans and rhesus macaques. Differences in immune cell frequencies as well as their expression profiles have been previously reported in both murine and non-human primate models (30, 44-46);

however, this has not served as a limitation, at least in the context of chronic infections, where many findings in mice and rhesus macaques have been applicable to human studies (12, 29, 34, 35). Nevertheless, further investigations of TIM-3 will be required to make any conclusion about these differences, especially given that the expression of TIM-3 on other lineages than T cells has comparatively been understudied.

Of the immune cell populations analyzed, mDCs represent the population with the most similar levels of TIM-3 expression between humans and rhesus macaques. Given the role of mDCs in modulating T cell function through activation and inhibitory signaling, we wanted to characterize this population. Our gating strategy included PD-L2, a ligand to PD-1 that has been shown to inhibit T cell activation and function (37). Surprisingly, we found that TIM-3 and PD-L2 defined two distinct and largely non-overlapping mDC populations. Reports of TIM-3 function on DCs have been limited and contradictory, whereby TIM-3 was proposed to play a role in DC activation (36). In contrast, another report implicates TIM-3 in DC inhibition where stimulated TIM-3-deficient DCs have a more robust cytokine expression profile than wild-type DCs (47).

How TIM-3 regulates the state of DC activation needs to be clarified, but we proceeded to further characterize these TIM-3 expressing mDCs. TIM-3^{+}PD-L2^{-} mDCs appeared to represent a more mature and activated mDC population than TIM-3^{-}PD-L2^{+} mDCs (38, 39). Not surprisingly, longitudinal monitoring of CD86 expression on mDCs of SIV-infected rhesus macaques revealed an overall increased frequency of CD86 expressing TIM-3^{+} mDCs. This led us to speculate that the presence of SIV antigen either directly or indirectly stimulated the activation of TIM-3^{+} mDCs, contributing to the overall immune inflammation.

Activation and maturation of DCs require danger signals either from proinflammatory cytokines (indirect) secreted by other immune cells or from bacterial or viral components (direct) recognized by the Toll-like receptors (TLRs) (1). In turn, TLR recognition on DCs induces proinflammatory cytokine production and enhanced antigen presentation to naïve T cells, ultimately resulting in an antigen-specific adaptive immune response. We therefore examined the TLR-3-dependent response of DCs to double-stranded RNA (dsRNA) and observed TIM-3 expressing mDCs respond to TLR-3 agonist, not TLR-4 agonist, with the production of TNF-α. This specific response to TLR-3 agonist supports the idea that these TIM-3$^+$ mDCs are the ones that are triggered during viral infection. Though retroviruses such as HIV and SIV represent single-strand RNA (ssRNA) viruses, the HIV genome contains domains with secondary structures that facilitate the formation of a duplex that can interact with dsRNA-binding proteins (48, 49), which suggests binding to TLR-3. The maturation of DCs plays an important role in generating acquired immunity and dsRNA, a molecular signature of viral infection, interacts with TLR-3 to induce a DC-dependent cytotoxic T cell response and overall antiviral protection (50, 51), yet the poor induction of IL-12 also suggest that the T/NK effector cell response elicited by such mDCs will be less effective in containing the virus not to mention that the production of TNF-α is likely to fuel the viral replication in vivo.

It was previously shown that the TIM-3 ligand, galectin-9, positively correlates with plasma HIV RNA levels and remains elevated in HIV-1 infected individuals despite antiretroviral treatment or elite controller status (52). We explored the possibility that the increase in frequency of TIM-3$^+$CD86$^+$ mDCs over the duration of infection may derive from an increase in galectin-9 as well. Examination of galectin-9 levels in plasma revealed SIV-

infected non-controllers had the highest levels, followed by SIV-infected elite-controllers, and then naïve rhesus macaques. Longitudinal analyses of chronically SIV-infected non-controllers revealed a significant surge in galectin-9 levels that remained constant throughout the study. The same can be observed for SIV-infected elite-controllers though galectin-9 was at significantly lower levels. Altogether, these conditions may result in galectin-9 mediated activation of TIM-3 expressing mDCs. Previous studies supports this idea by showing galectin-9 promotes DC maturation (53), which expands a TIM-3$^+$ DC population that interacts with galectin-9 to promote the activation and proliferation of CD8$^+$ T cells, enhancing anti-tumor activity (36). Involvement of TIM-3 expressing mDCs in early viral infection and subsequent exposure to galectin-9 may lead to activating an antigen-specific T cell response.

Although the precise mechanism involving TIM-3 and its ligand(s) remain to be fully elucidated especially among the various cells of the immune system, we tested a novel TIM-3 blocking strategy, noting that antibody and soluble TIM-3 blockade of the TIM-3 pathway as well as PD-1 blockade has been shown to enhance function of exhausted virus-specific T cells (12, 29, 34, 35). However, commensurate with the low levels of TIM-3 expression on rhesus macaque T cells, restoration of antigen-specific T cell function was minimal in our pilot experiment, though the role of such blockade will need to be expanded to other cell lineages.

However, the TIM-3 Fc fusion protein generated provides a number of advantages for downstream applications including in vivo studies. TIM-3-Fc represents a homodimer with large molecular weight deriving from the disulfide bridging between the Fc regions fused to each TIM-3 molecule. As a result, this large TIM-3-Fc will not be rapidly cleared by

the kidney, and thus have a longer half-life that is comparable to antibodies (55, 56). The Fc region also mediates recycling via the FcRn salvage pathway, further increasing half-life. Much like antibody purification, Fc fusion purification can take advantage of Protein G Sepharose affinity chromatography to achieve ultra-pure product (57). Upon purification of TIM-3-Fc, we tested protein activity using galectin-9. Though TIM-3 has been described as a receptor for galectin-9, this notion has been challenged in a controversial study (40). In addition to producing TIM-3-Fc, we expressed the individual extracellular domains as IgV-Fc and mucin-Fc. The combined use of these Fc fusion proteins revealed galectin-9 binds to the TIM-3 IgV domain but not the mucin domain.

The R-phycoerythrin (R-PE) labeled TIM-3-Fc (TIM-3-Fc/R-PE), also represents an interesting probe to determine the expression of ligands on the surface and in cells. Staining revealed binding to various primary immune cells, amongst most prominent were monocytes and B cells. Our data also supports other ligands aside from galectin-9 binding to the TIM-3-Fc/R-PE, supporting previous studies that have noted various other ligands for TIM-3 besides galectin-9 (47, 58, 59). Though we and others provide evidence TIM-3 signaling contributes to DC maturation and activation (36), additional studies have suggested the existence of other unidentified TIM-3 ligands that bind to other domains of TIM-3 and exert other regulatory functions. Crystallography studies of the IgV domain of murine TIM-3 revealed a galectin-9 independent binding site (60), suggesting other ligands aside from galectin-9.

Our findings from staining with TIM-3-Fc/R-PE present two possibilities: (1) the identification of a new TIM-3 ligand expressing cell population; or even more exciting (2)

elucidation of a novel TIM-3 ligand. Future work will involve TIM-3-Fc pulldown assays to elucidate the identity of the ligand(s).

Future Directions

Before we proceed with using TIM-3-Fc as an immunotherapeutic in vivo, further assessment of TIM-3 blockade at various time-points as well as understanding of the mechanisms of inhibiting TIM-3 signaling will be required. Differences have been observed between acute and chronic infection with HIV, especially with T cell exhaustion (67). Though the exact mechanism underlying these differences are not well understood, it is clear we need to expand our focus from T cells to incorporate other immune cells, including mDCs, B cells, and NK cells, to fully grasp how TIM-3 influences overall immune exhaustion. One not reported finding is the fact that TIM-3 is rapidly downregulated on the surface of mDCs suggesting that functional evaluation will most likely require in vivo testing. Given the complexity of the TIM-3 pathway, future studies will focus on elucidating TIM-3 ligands to explore how TIM-3/TIM-3 ligand interactions mediate immune function.

Conclusion

In this study, we determined the expression of TIM-3 and TIM-3 ligand in SIV-infected rhesus macaques, finding that both molecules are expressed on a greater number of immune cell populations than previously thought. We focused on a newly defined population of TIM-3 expressing mDCs, observing expression and secretion of TNF-α in a TLR-3-dependent manner to dsRNA. Our findings from this study will be important to understanding the dualistic nature of TIM-3 as both an activation marker for innate immunity while also an inhibitory marker for adaptive immunity. Our ultimate goal is to determine whether TIM-3-Fc may be of clinical benefit and in what situations. In spite of the reported differences in expression on various lineages, the macaque model will greatly facilitate these studies to test whether a clinical translation may be justified.

References

1. Medzhitov, R., and C. Janeway. 2000. Innate Immunity. *New England Journal of Medicine* 343: 338-344.
2. Ravetch, J. V., and L. L. Lanier. 2000. Immune Inhibitory Receptors. *Science* 290: 84-89.
3. Lanier, L. L., S. O'Fallon, C. Somoza, J. H. Phillips, P. S. Linsley, K. Okumura, D. Ito, and M. Azuma. 1995. CD80 (B7) and CD86 (B70) provide similar costimulatory signals for T cell proliferation, cytokine production, and generation of CTL. *Journal of Immunology* 154: 97-105.
4. Wherry, E. J. 2011. T cell exhaustion. *Nature Immunology* 12: 492-499.
5. Linsley, P. S., J. L. Greene, W. Brady, J. Bajorath, J. A. Ledbetter, and R. Peach. 1994. Human B7-1 (CD80) and B7-2 (CD86) bind with similar avidities but distinct kinetics to CD28 and CTLA-4 receptors. *Immunity* 1: 793-801.
6. van der Merwe, P. A., D. L. Bodian, S. Daenke, P. Linsley, and S. J. Davis. 1997. CD80 (B7-1) Binds Both CD28 and CTLA-4 with a Low Affinity and Very Fast Kinetics. *Journal of Experimental Medicine* 185: 393-404.
7. Judge, T. A., Z. Wu, X. G. Zheng, A. H. Sharpe, M. H. Sayegh, and L. A. Turka. 1999. The role of CD80, CD86, and CTLA4 in alloimmune responses and the induction of long-term allograft survival. *Journal of Immunology* 162: 1947-1951.
8. Barber, D. L., E. J. Wherry, D. Masopust, B. Zhu, J. P. Allison, A. H. Sharpe, G. J. Freeman, and R. Ahmed. 2006. Restoring function in exhausted CD8 T cells during chronic viral infection. *Nature* 439: 682-687.

9. Kaufmann, D. E., D. G. Kavanagh, F. Pereyra, J. J. Zaunders, E. W. Mackey, T. Miura, S. Palmer, M. Brockman, A. Rathod, A. Piechocka-Trocha, B. Baker, B. Zhu, S. Le Gall, M. T. Waring, R. Ahern, K. Moss, A. D. Kelleher, J. M. Coffin, G. J. Freeman, E. S. Rosenberg, and B. D. Walker. 2007. Upregulation of CTLA-4 by HIV-specific CD4+ T cells correlates with disease progression and defines a reversible immune dysfunction. *Nature Immunology* 8: 1246-1254.

10. Watanabe, N., M. Gavrieli, J. R. Sedy, J. Yang, F. Fallarino, S. K. Loftin, M. A. Hurchla, N. Zimmerman, J. Sim, X. Zang, T. L. Murphy, J. H. Russell, J. P. Allison, and K. M. Murphy. 2003. BTLA is a lymphocyte inhibitory receptor with similarities to CTLA-4 and PD-1. *Nature Immunology* 4: 670-679.

11. Woo, S.-R., M. E. Turnis, M. V. Goldberg, J. Bankoti, M. Selby, C. J. Nirschl, M. L. Bettini, D. M. Gravano, P. Vogel, C. L. Liu, S. Tangsombatvisit, J. F. Grosso, G. Netto, M. P. Smeltzer, A. Chaux, P. J. Utz, C. J. Workman, D. M. Pardoll, A. J. Korman, C. G. Drake, and D. A. A. Vignali. 2012. Immune Inhibitory Molecules LAG-3 and PD-1 Synergistically Regulate T-cell Function to Promote Tumoral Immune Escape. *Cancer Research* 72: 917-927.

12. Jones, R. B., L. C. Ndhlovu, J. D. Barbour, P. M. Sheth, A. R. Jha, B. R. Long, J. C. Wong, M. Satkunarajah, M. Schweneker, J. M. Chapman, G. Gyenes, B. Vali, M. D. Hyrcza, F. Y. Yue, C. Kovacs, A. Sassi, M. Loutfy, R. Halpenny, D. Persad, G. Spotts, F. M. Hecht, T.-W. Chun, J. M. McCune, R. Kaul, J. M. Rini, D. F. Nixon, and M. A. Ostrowski. 2008. Tim-3 expression defines a novel population of dysfunctional T cells with highly elevated frequencies in progressive HIV-1 infection. *Journal of Experimental Medicine* 205: 2763-2779.

13. Bengsch, B., B. Seigel, M. Ruhl, J. Timm, M. Kuntz, H. E. Blum, H. Pircher, and R. Thimme. 2010. Coexpression of PD-1, 2B4, CD160 and KLRG1 on Exhausted HCV-Specific CD8+ T Cells Is Linked to Antigen Recognition and T Cell Differentiation. *PLoS Pathogen* 6: e1000947.

14. Blackburn, S. D., H. Shin, W. N. Haining, T. Zou, C. J. Workman, A. Polley, M. R. Betts, G. J. Freeman, D. A. A. Vignali, and E. J. Wherry. 2009. Coregulation of CD8+ T cell exhaustion by multiple inhibitory receptors during chronic viral infection. *Nature Immunology* 10: 29-37.

15. Monney, L., C. A. Sabatos, J. L. Gaglia, A. Ryu, H. Waldner, T. Chernova, S. Manning, E. A. Greenfield, A. J. Coyle, R. A. Sobel, G. J. Freeman, and V. K. Kuchroo. 2002. Th1-specific cell surface protein Tim-3 regulates macrophage activation and severity of an autoimmune disease. *Nature* 415: 536-541.

16. Sanchez-Fueyo, A., J. Tian, D. Picarella, C. Domenig, X. X. Zheng, C. A. Sabatos, N. Manlongat, O. Bender, T. Kamradt, V. K. Kuchroo, J.-C. Gutierrez-Ramos, A. J. Coyle, and T. B. Strom. 2003. Tim-3 inhibits T helper type 1-mediated auto- and alloimmune responses and promotes immunological tolerance. *Nature Immunology* 4: 1093-1101.

17. Sabatos, C. A., S. Chakravarti, E. Cha, A. Schubart, A. Sanchez-Fueyo, X. X. Zheng, A. J. Coyle, T. B. Strom, G. J. Freeman, and V. K. Kuchroo. 2003. Interaction of Tim-3 and Tim-3 ligand regulates T helper type 1 responses and induction of peripheral tolerance. *Nature Immunology* 4: 1102-1110.

18. Zhu, C., A. C. Anderson, A. Schubart, H. Xiong, J. Imitola, S. J. Khoury, X. X. Zheng, T. B. Strom, and V. K. Kuchroo. 2005. The Tim-3 ligand galectin-9 negatively regulates T helper type 1 immunity. *Nature Immunology* 6: 1245-1252.

19. Wang, F., L. Wan, C. Zhang, X. Zheng, J. Li, and Z. K. Chen. 2009. Tim-3-Galectin-9 pathway involves the suppression induced by CD4+CD25+ regulatory T cells. *Immunobiology* 214: 342-349.

20. Oomizu, S., T. Arikawa, T. Niki, T. Kadowaki, M. Ueno, N. Nishi, A. Yamauchi, T. Hattori, T. Masaki, and M. Hirashima. 2012. Cell Surface Galectin-9 Expressing Th Cells Regulate Th17 and Foxp3+ Treg Development by Galectin-9 Secretion. *PLoS ONE* 7: e48574.

21. Vali, B., R. B. Jones, A. Sakhdari, P. M. Sheth, K. Clayton, F. Y. Yue, G. Gyenes, D. Wong, M. B. Klein, S. Saeed, E. Benko, C. Kovacs, R. Kaul, and M. A. Ostrowski. 2010. HCV-specific T cells in HCV/HIV co-infection show elevated frequencies of dual Tim-3/PD-1 expression that correlate with liver disease progression. *European Journal of Immunology* 40: 2493-2505.

22. Sakhdari, A., S. Mujib, B. Vali, F. Y. Yue, S. MacParland, K. Clayton, R. B. Jones, J. Liu, E. Y. Lee, E. Benko, C. Kovacs, J. Gommerman, R. Kaul, and M. A. Ostrowski. 2012. Tim-3 Negatively Regulates Cytotoxicity in Exhausted CD8+ T Cells in HIV Infection. *PLoS ONE* 7: e40146.

23. Nebbia, G., D. Peppa, A. Schurich, P. Khanna, H. D. Singh, Y. Cheng, W. Rosenberg, G. Dusheiko, R. Gilson, J. ChinAleong, P. Kennedy, and M. K. Maini. 2012. Upregulation of the Tim-3/Galectin-9 Pathway of T Cell Exhaustion in Chronic Hepatitis B Virus Infection. *PLoS ONE* 7: e47648.

24. Wu, W., Y. Shi, S. Li, Y. Zhang, Y. Liu, Y. Wu, and Z. Chen. 2012. Blockade of Tim-3 signaling restores the virus-specific CD8+ T-cell response in patients with chronic hepatitis B. *European Journal of Immunology* 42: 1180-1191.

25. McMahan, R. H., L. Golden-Mason, M. I. Nishimura, B. J. McMahon, M. Kemper, T. M. Allen, D. R. Gretch, and H. R. Rosen. 2010. Tim-3 expression on PD-1+ HCV-specific human CTLs is associated with viral persistence, and its blockade restores hepatocyte-directed in vitro cytotoxicity. *Journal of Clinical Investigation* 120: 4546-4557.

26. Golden-Mason, L., B. E. Palmer, N. Kassam, L. Townshend-Bulson, S. Livingston, B. J. McMahon, N. Castelblanco, V. Kuchroo, D. R. Gretch, and H. R. Rosen. 2009. Negative Immune Regulator Tim-3 Is Overexpressed on T Cells in Hepatitis C Virus Infection and Its Blockade Rescues Dysfunctional CD4+ and CD8+ T Cells. *Journal of Virology* 83: 9122-9130.

27. Ju, Y., N. Hou, X. N. Zhang, D. Zhao, Y. Liu, J. J. Wang, F. Luan, W. Shi, F. L. Zhu, W. S. Sun, L. N. Zhang, C. J. Gao, L. F. Gao, X. H. Liang, and C. H. Ma. 2009. Blockade of Tim-3 pathway ameliorates interferon-gamma production from hepatic CD8+ T cells in a mouse model of hepatitis B virus infection. *Cellular and Molecular Immunology* 6: 35-43.

28. Sehrawat, S., P. B. J. Reddy, N. Rajasagi, A. Suryawanshi, M. Hirashima, and B. T. Rouse. 2010. Galectin-9/TIM-3 Interaction Regulates Virus-Specific Primary and Memory CD8+ T Cell Response. *PLoS Pathogen* 6: e1000882.

29. Jin, H.-T., A. C. Anderson, W. G. Tan, E. E. West, S.-J. Ha, K. Araki, G. J. Freeman, V. K. Kuchroo, and R. Ahmed. 2010. Cooperation of Tim-3 and PD-1 in CD8 T-cell

exhaustion during chronic viral infection. *Proceedings of the National Academy of Sciences* 107: 14733-14738.

30. Amancha, P. K., J. J. Hong, A. A. Ansari, and F. Villinger. 2015. Up-regulation of Tim-3 on T cells during acute simian immunodeficiency virus infection and on antigen specific responders. *AIDS* 29: 531-536.

31. Fujita, T., B. J. Burwitz, G. M. Chew, J. S. Reed, R. Pathak, E. Seger, K. L. Clayton, J. M. Rini, M. A. Ostrowski, N. Ishii, M. J. Kuroda, S. G. Hansen, J. B. Sacha, and L. C. Ndhlovu. 2014. Expansion of dysfunctional Tim-3-expressing effector memory CD8+ T cells during simian immunodeficiency virus infection in rhesus macaques. *Journal of Immunology* 193: 5576-5583.

32. Mujib, S., R. B. Jones, C. Lo, N. Aidarus, K. Clayton, A. Sakhdari, E. Benko, C. Kovacs, and M. A. Ostrowski. 2012. Antigen-independent induction of Tim-3 expression on human T cells by the common gamma-chain cytokines IL-2, IL-7, IL-15, and IL-21 is associated with proliferation and is dependent on the phosphoinositide 3-kinase pathway. *Journal of Immunology* 188: 3745-3756.

33. Haase, A. T. 2005. Perils at mucosal front lines for HIV and SIV and their hosts. *Nature Reviews Immunology* 5: 783-792.

34. Velu, V., K. Titanji, B. Zhu, S. Husain, A. Pladevega, L. Lai, T. H. Vanderford, L. Chennareddi, G. Silvestri, G. J. Freeman, R. Ahmed, and R. R. Amara. 2009. Enhancing SIV-specific immunity in vivo by PD-1 blockade. *Nature* 458: 206-210.

35. Amancha, P. K., J. J. Hong, K. Rogers, A. A. Ansari, and F. Villinger. 2013. In vivo blockade of the programmed cell death-1 pathway using soluble recombinant PD-1-

Fc enhances CD4+ and CD8+ T cell responses but has limited clinical benefit. *Journal of Immunology* 191: 6060-6070.

36. Nagahara, K., T. Arikawa, S. Oomizu, K. Kontani, A. Nobumoto, H. Tateno, K. Watanabe, T. Niki, S. Katoh, M. Miyake, S. Nagahata, J. Hirabayashi, V. K. Kuchroo, A. Yamauchi, and M. Hirashima. 2008. Galectin-9 increases Tim-3+ dendritic cells and CD8+ T cells and enhances antitumor immunity via galectin-9-Tim-3 interactions. *Journal of Immunology* 181: 7660-7669.

37. Latchman, Y., C. R. Wood, T. Chernova, D. Chaudhary, M. Borde, I. Chernova, Y. Iwai, A. J. Long, J. A. Brown, R. Nunes, E. A. Greenfield, K. Bourque, V. A. Boussiotis, L. L. Carter, B. M. Carreno, N. Malenkovich, H. Nishimura, T. Okazaki, T. Honjo, A. H. Sharpe, and G. J. Freeman. 2001. PD-L2 is a second ligand for PD-1 and inhibits T cell activation. *Nature Immunology* 2: 261-268.

38. Tan, J. K., and H. C. O'Neill. 2005. Maturation requirements for dendritic cells in T cell stimulation leading to tolerance versus immunity. *Journal of Leukocyte Biology* 78: 319-324.

39. Loré, K., A. Sönnerborg, C. Broström, L.-E. Goh, L. Perrin, H. McDade, H.-J. Stellbrink, B. Gazzard, R. Weber, L. A. Napolitano, Y. van Kooyk, and J. Andersson. 2002. Accumulation of DC-SIGN+CD40+ dendritic cells with reduced CD80 and CD86 expression in lymphoid tissue during acute HIV-1 infection. *AIDS* 16: 683-692.

40. Leitner, J., A. Rieger, W. F. Pickl, G. Zlabinger, K. Grabmeier-Pfistershammer, and P. Steinberger. 2013. TIM-3 Does Not Act as a Receptor for Galectin-9. *PLoS Pathogen* 9: e1003253.

41. Onlamoon, N., K. Rogers, A. E. Mayne, K. Pattanapanyasat, K. Mori, F. Villinger, and A. A. Ansari. 2008. Soluble PD-1 rescues the proliferative response of simian immunodeficiency virus-specific CD4 and CD8 T cells during chronic infection. *Immunology* 124: 277-293.

42. Johansson, D. X., K. Drakenberg, K. H. Hopmann, A. Schmidt, F. Yari, J. Hinkula, and M. A. A. Persson. 2007. Efficient expression of recombinant human monoclonal antibodies in Drosophila S2 cells. *Journal of Immunological Methods* 318: 37-46.

43. Tieu, R., P. K. Amancha, F. Villinger, and S. N. Byrareddy. 2014. TIM-3, a Possible Target for Immunotherapy in Cancer and Chronic Viral Infections. *Austin Virology and Retrovirology* 1: 6.

44. Ito, R., T. Takahashi, I. Katano, and M. Ito. 2012. Current advances in humanized mouse models. *Cellular and Molecular Immunology* 9: 208-214.

45. Mestas, J., and C. C. Hughes. 2004. Of Mice and Not Men: Differences between Mouse and Human Immunology. *Journal of Immunology* 172: 2731-2738.

46. Pitcher, C. J., S. I. Hagen, J. M. Walker, R. Lum, B. L. Mitchell, V. C. Maino, M. K. Axthelm, and L. J. Picker. 2002. Development and Homeostasis of T Cell Memory in Rhesus Macaque. *Journal of Immunology* 168: 29-43.

47. Chiba, S., M. Baghdadi, H. Akiba, H. Yoshiyama, I. Kinoshita, H. Dosaka-Akita, Y. Fujioka, Y. Ohba, J. V. Gorman, J. D. Colgan, M. Hirashima, T. Uede, A. Takaoka, H. Yagita, and M. Jinushi. 2012. Tumor-infiltrating DCs suppress nucleic acid-mediated innate immune responses through interactions between the receptor TIM-3 and the alarmin HMGB1. *Nature Immunology* 13: 832-842.

48. Windbichler, N., M. Werner, and R. Schroeder. 2003. Kissing complex-mediated dimerisation of HIV-1 RNA: coupling extended duplex formation to ribozyme cleavage. *Nucleic Acids Research* 31: 6419-6427.

49. Bernacchi, S., E. Ennifar, K. Toth, P. Walter, J. Langowski, and P. Dumas. 2005. Mechanism of hairpin-duplex conversion for the HIV-1 dimerization initiation site. *Journal of Biological Chemistry* 280: 40112-40121.

50. Jelinek, I., J. N. Leonard, G. E. Price, K. N. Brown, A. Meyer-Manlapat, P. K. Goldsmith, Y. Wang, D. Venzon, S. L. Epstein, and D. M. Segal. 2011. TLR3-Specific Double-Stranded RNA Oligonucleotide Adjuvants Induce Dendritic Cell Cross-Presentation, CTL Responses, and Antiviral Protection. *Journal of Immunology* 186: 2422-2429.

51. Alexopoulou, L., A. C. Holt, R. Medzhitov, and R. A. Flavell. 2001. Recognition of double-stranded RNA and activation of NF-kappa B by Toll-like receptor 3. *Nature* 413: 732-738.

52. Tandon, R., G. M. Chew, M. M. Byron, P. Borrow, T. Niki, M. Hirashima, J. D. Barbour, P. J. Norris, M. C. Lanteri, J. N. Martin, S. G. Deeks, and L. C. Ndhlovu. 2014. Galectin-9 Is Rapidly Released During Acute HIV-1 Infection and Remains Sustained at High Levels Despite Viral Suppression Even in Elite Controllers. *AIDS Research and Human Retroviruses* 30: 654-664.

53. Dai, S. Y., R. Nakagawa, A. Itoh, H. Murakami, Y. Kashio, H. Abe, S. Katoh, K. Kontani, M. Kihara, S. L. Zhang, T. Hata, T. Nakamura, A. Yamauchi, and M. Hirashima. 2005. Galectin-9 Induces Maturation of Human Monocyte-Derived Dendritic Cells. *Journal of Immunology* 175: 2974-2981.

54. Anc, W., A. Nesbitt, A. P. Chapman, A. G. P. P. Antoniw, and A. D. G. Lawson. 2002. Formatting antibody fragments to mediate specific therapeutic functions. *Biochemical Society Transactions* 30.

55. Wang, W., E. Q. Wang, and J. P. Balthasar. 2008. Monoclonal Antibody Pharmacokinetics and Pharmacodynamics. *Clinical Pharmacology & Therapeutics* 84: 548-558.

56. Jungabauer, A., C. Tauer, M. Reiter, M. Purtscher, E. Wenisch, F. Steindl, A. Buchacher, and H. Katinger. 1989. Comparison of protein A, protein G and copolymerized hydroxyapatite for the purification of human monoclonal antibodies. *Journal of Chromatography A* 476: 257-268.

57. Nakayama, M., H. Akiba, K. Takeda, Y. Kojima, M. Hashiguchi, M. Azuma, H. Yagita, and K. Okumura. 2009. Tim-3 mediates phagocytosis of apoptotic cells and cross-presentation. *Blood* 113: 3821-3830.

58. Huang, Y.-H., C. Zhu, Y. Kondo, A. C. Anderson, A. Gandhi, A. Russell, S. K. Dougan, B.-S. Petersen, E. Melum, T. Pertel, K. L. Clayton, M. Raab, Q. Chen, N. Beauchemin, P. J. Yazaki, M. Pyzik, M. A. Ostrowski, J. N. Glickman, C. E. Rudd, H. L. Ploegh, A. Franke, G. A. Petsko, V. K. Kuchroo, and R. S. Blumberg. 2015. CEACAM1 regulates TIM–3–mediated tolerance and exhaustion. *Nature* 517: 386-390.

59. Cao, E., X. Zang, U. A. Ramagopal, A. Mukhopadhaya, A. Fedorov, E. Fedorov, W. D. Zencheck, J. W. Lary, J. L. Cole, H. Deng, H. Xiao, T. P. Dilorenzo, J. P. Allison, S. G. Nathenson, and S. C. Almo. 2007. T Cell Immunoglobulin Mucin-3 Crystal Structure Reveals A Galectin-9-Independent Ligand-Binding Surface. *Immunity* 26: 311-321.

60. Goulder, P. J. R., M. A. Altfeld, E. S. Rosenberg, T. Nguyen, Y. Tang, R. L. Eldridge, M. M. Addo, S. He, J. S. Muckerjee, M. N. Phillips, M. Bunce, S. A. Kalams, R. P. Sekaly, B. D. Walker, and C. Brander. 2001. Substantial Differences in Specificity of HIV-Specific Cytotoxic T Cells in Acute and Chronic HIV Infection. *Journal of Experimental Medicine* 193: 181-194.